Nanostructured lipid carriers as a delivery system of tobramycin and ciprofloxacin: preparation, testing and validation in the *Caenorhabditis elegans* model

Vera Lúcia Ribeiro Esgueira

Thesis to obtain the Master of Science Degree in

Biotechnology

Supervisors: Professor Luís Joaquim Pina da Fonseca
Professor Jorge Humberto Gomes Leitão

Examination Committee

Chairperson: Professor Helena Maria Rodrigues Vasconcelos Pinheiro
Supervisor: Professor Luís Joaquim Pina da Fonseca
Members of the Committee: Doctor Dragana Popovic Correia de Barros

November 2017

Agradecimentos

Em primeiro lugar quero agradecer aos meus orientadores por me terem aceite neste tema e disponibilizado todos os meios para desenvolver esta tese.

Quero também agradecer à Ana Catarina e Fátima Pinto por terem partilhado comigo todo o conhecimento sobre nanopartículas lipídicas e pela ajuda no laboratório no desenvolvimento das mesmas.

À Joana Feliciano e Sílvia Sousa por me terem ajudado com os ensaios biológicos, por terem partilhado comigo todas as informações sobre o modelo animal *C. elegans*, e por terem sempre sugestões enriquecedoras.

À Ana Pfluck, por toda a ajuda no laboratório e por todo o apoio ao longo do desenvolvimento desta tese.

A todas as pessoas maravilhosas que conheci nos laboratórios onde trabalhei, obrigada pela boa disposição e espírito de equipa.

A toda a minha turma do mestrado em Biotecnologia, sem vocês este curso não teria sido o mesmo.

Um agradecimento especial ao Pedro Silva por todo o apoio e carinho.

A todos os meus amigos, pelo apoio durante os últimos anos e especialmente durante este período.

Finalmente quero agradecer à minha família por todo o apoio e compreensão demonstrado nestes últimos tempos.

Obrigado a todos!!

Abstract

In this work, a nanostructured lipid carrier (NLC) formulation was developed, optimized and characterized, followed by the encapsulation of two antibiotics currently used in cystic fibrosis therapy, ciprofloxacin and tobramycin.

Different oils, fatty acids and surfactants were tested. Average size of nanoparticles ranged from 668.1±232.6 to 202.4±2.7nm while their polydispersity index (PdI) ranged from 0.840±0.08 to 0.208±0.03 and zeta potential (ZP) ranged from -20.3±0.52 to -56.9±3.72mV. The formulation chosen for the encapsulation of the antibiotics were composed of stearic acid, sunflower oil, span 80 and milli-Q water. Empty nanoparticles had an average size of 255.9±40.8nm, PdI of 0.342±0.06 and ZP of -56.9±3.72mV. Nanoparticles with ciprofloxacin and tobramycin exhibited a similar average size compared to empty nanoparticles. Zeta potential of nanoparticles with tobramycin was much lower than that of empty nanoparticles, suggesting that these nanoparticles are long-term instable. Thermal analysis showed a melting temperature of 58.9ºC±2.25ºC, 59.5±0.05ºC and 56.9±0.30ºC for empty nanoparticles, nanoparticles with ciprofloxacin, and nanoparticles with tobramycin, respectively. Transmission electron microscopy provided images of nanoparticles with spherical shape and with a size of approximately 200 nm.

In suspension, empty nanoparticles and nanoparticles with ciprofloxacin were stable up two months in opposition to nanoparticles with tobramycin.

Nanoparticles with ciprofloxacin had an encapsulation efficiency of 68.16±4.9% and a burst release where all the drug was released in the first 7 hours.

The efficacy of encapsulated antibiotics was assessed using *Caenorhabditis elegans* as an animal model of infection and bacterial pathogens *Burkholderia contaminans* IST408 and *Burkholderia cenocepacia* K56-2, as model pathogens. The significantly difference was observed in the survival of *C. elegans* infected with *B. contaminans* IST408 upon exposure between nanoparticles with ciprofloxacin or without nanoparticles (p-value<0.05) and between empty nanoparticles or nanoparticles with antibiotic (p-value<0.01). For *C. elegans* infected with *B. cenocepacia* K56-2 no significant difference in survival was observed when worms were fed with nanoparticles with antibiotic.

Key words: Nanostructured lipid carriers, Ciprofloxacin, Tobramycin, *C. elegans*

Resumo

Neste trabalho, foi desenvolvida, otimizada e caracterizada uma formulação de vetores lipídicos nanoestruturados, seguido da encapsulação de dois antibióticos (tobramicina e ciprofloxacina) atualmente usados na terapia da fibrose quística.

Diferentes óleos, ácidos gordos e surfactantes foram testados. O tamanho médio das nanopartículas obtidas variou de 668.1±232.6 a 202.4±2.7nm, enquanto que o índice de polidispersão variou de 0.840±0.08 a 0.208±0.03 e o potencial zeta variou de -20.3±0.52 a -56.9±3.72mV. A formulação escolhida para a encapsulação dos antibióticos foi constituída por ácido esteárico, óleo de girassol, Span 80 e água milli-Q. As nanopartículas vazias obtidas tiveram um tamanho médio de 255.9±40.8nm, índice de polidispersão de 0.342±0.06 e um potencial zeta de -56.9±3.72mV. As nanopartículas com os antibióticos encapsulados tiveram um tamanho e um índice de polidispersão similar às nanopartículas vazias. O potencial zeta das nanopartículas com tobramicina foi muito inferior ao obtido nas nanopartículas vazias, sugerindo que estas são instáveis a longo prazo. A análise termal das nanopartículas mostrou uma temperatura de fusão de 58.9ºC±2.25ºC, 59.5±0.05ºC e 56.9±0.30ºC para nanopartículas vazias, nanopartículas com ciprofloxacina e nanopartículas com tobramicina, respetivamente. Imagens de microscopia de transmissão eletrónica mostraram partículas com forma esférica e com tamanho de aproximadamente 200 nm.

Em suspensão, as nanopartículas vazias e com ciprofloxacina mostraram-se estáveis até dois meses, em oposição às nanopartículas com tobramicina.

Nanopartículas com ciprofloxacina tiveram uma eficiência de encapsulação de 68.16±4.9% e uma libertação rápida do fármaco onde este foi libertado nas primeiras 7 horas.

A eficácia da ciprofloxacina encapsulada em nanopartículas lipídicas foi avaliada usando *C. elegans* como modelo animal de infeção, e *Burkholderia contaminans* IST408 e *Burkholderia cenocepacia* K56-2 como bactérias patogénicas. A maior diferença foi observada na sobrevivência de *C. elegans* infetados com *B. contaminans* IST408 expostos a nanopartículas com ciprofloxacina ou sem nanopartículas (*p-value*<0.05) e entre nanopartículas vazias e nanopartículas com ciprofloxacina (*p-value*<0.01). No caso de *C. elegans* infetado com *B. cenocepacia* K56-2 não foi observada diferença na sobrevivência quando o nematode foi alimentado com nanopartículas com ciprofloxacina.

Palavras-chave: Vetores lipídicos nanoestruturados, Ciprofloxacina, Tobramicina, *C. elegans*

Table of contents

List of figures

List of tables

Abbreviations

AFM - Atomic force microscopy

CMC - Critical micelle concentration

CF - Cystic fibrosis

CFTR - Cystic fibrosis transmembrane conductance regulator

DL - Drug loading capacity

DLS - Dynamic light scattering

DSC - Differential scanning calorimetry

EE - Encapsulation efficiency

FDA - Food and drug administration

HLB - Hydrophile-lipophile balance

HPLC - High-performance liquid chromatography

HSM CF Center - Hospital Santa Maria cystic fibrosis center

LDC - Lipid drug conjugates

LD - Laser diffraction

MDR - Multidrug desistance

MIC - Minimal inhibitory concentration

NLC - Nanostructured lipid carrier

O/W - Oil-in-Water

PdI - Polydispersity index

PSC - Photon correlation spectroscopy

SD - Standard deviation

SEM - Scanning electron microscopy

SLN - Solid lipid nanoparticle

RP-HPLC - Reverse phase high performance liquid chromatography

TEM - Transmission electron microscopy

ZP - Zeta potential

UV-Vis - Ultraviolet-visible

W/O - Water-in-Oil

W/O/W - Water-in-oil-in-water

1. Introduction

1.1. Lipid nanoparticles

Lipid drug carriers have been investigated for years and include oil-in-water (o/w) emulsions, liposomes, microparticles and nanoparticles[1]. First lipid particle, a fat emulsion, was developed for parenteral nutrition in the 1960s by Wrethind. Lipophilic drugs can be easily incorporated in the oil droplets but have the disadvantage of low physical stability, which can lead to agglomeration or breaking of the emulsion[2].

Liposomes are spherical vesicles composed of phospholipids arranged in sheets that form a bilayer membrane. Liposomes were described in the 1960s by Bangham and used as drug delivery vehicles in the 1970s. In 1986, liposomes entered in to the cosmetic market. These carrier systems have some disadvantages such as physical stability of the dispersion, drug leakage, low activity and difficulties in upscaling[1–3].

In the middle of the 1990s a new alternative for traditional colloidal carriers made from solid lipids emerged. They were called solid lipid nanoparticles (SLN). Some modified SLN have been developed such as nanostructured lipid carriers (NLC) and the lipid drug conjugates (LDC). These new carriers overcame some limitations of SLN[2].

Typical structures of liposomes, nanoemulsions, solid lipid nanoparticles and nanostructured lipid carriers are schematically represented in figure 1.
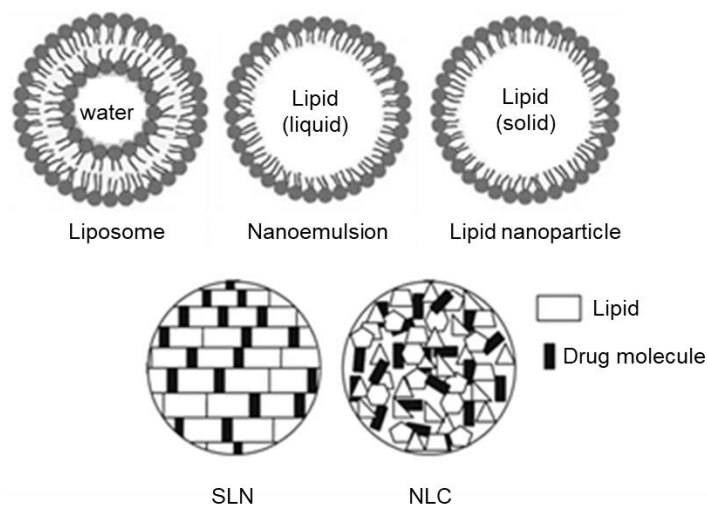
Figure 1: Structure of liposomes, nanoemulsions, solid lipid nanoparticles (SLNs) and nanostructured lipid carriers (NLC). Adapted from[4,5].

1.1.1. Solid lipid nanoparticles

Solid lipid nanoparticles are colloidal dispersions with a solid matrix composed of biodegradable lipids, emulsifiers (to stabilize the lipid dispersion) and water, with a mean diameter ranging from 50 to

1000nm. These lipids include triglycerides, fatty acids, steroids and waxes. They are prepared from lipids which are solid at room temperature as well as at body temperature[4,6,7].

Compared to liposomes and emulsions, solid nanoparticles combine the advantage of physical stability, protection of the incorporated drug from degradation, and controlled release. They can be applied in various applications such as parenteral, oral, dermal, ocular, pulmonary and rectal[2,8].

Solid lipid nanoparticles have some limitations. The main disadvantages of this system include poor drug loading capacity, drug expulsion after polymeric transition during storage and relative high water content of the dispersion (70-99%)[7].

There are three different models for the incorporation of drugs in the SLNs. These include the homogeneous matrix model, the drug-enriched shell model, and the drug-enriched core model (Figure 2). Those structures depend on the lipid content of the formulation and production conditions. A homogeneous matrix is obtained with cold homogenisation method and, when drugs to be incorporated are very lipophilic, with hot homogenisation. An outer shell enriched with drug is obtained when phase separation occurs during the cooling process from the liquid oil droplet to the formation of a solid particle where the lipid precipitate first formatting a nearly compound-free lipid core. A core enriched with drug is formed when the drug starts precipitating first and consequently the shell will contain lower amounts of drug. This last model allows a better control of drug release[1,2,8].
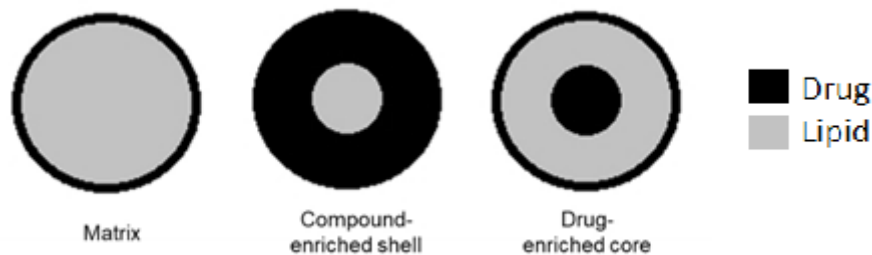
Figure 2: Models of incorporation of drugs in solid lipid nanoparticles. Adapted from[8].

1.1.2. Nanostructured lipid carriers

Nanostructured lipid carriers, as previously mentioned, are systems that minimise or avoid some potential problems associated with SLNs. These problems include drug expulsion during storage and low pay-load for several drugs. For the NLCs production different solid lipid molecules at room temperature are mixed with liquid lipid (oil). The resulting particle shows a lower melting point compared to SLNs but is still solid at body temperature. There are three different types of NLC, multiple type, amorphous type and imperfect type (figure 3).
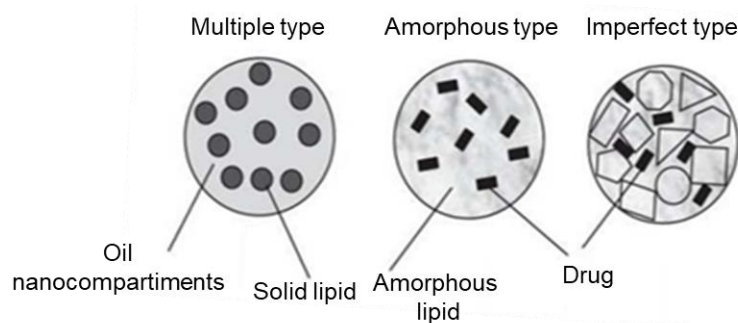
Figure 3: The three types of NLCs, imperfect type, amorphous type and multiple type. Adapted from[9].

The imperfect type is obtained by using different molecules to build a matrix that leaves enough imperfections to incorporate drugs. The amorphous type is obtained by a solid lipid matrix but not crystalline, which avoids the drug expulsion that can occur in SLNs. The multiple type is similar to oil emulsion but with oil-in-solid and lipid-in-water dispersion where the solid lipid matrix contains tiny nanocompartments. This last NLC type has the advantage of incorporating drugs that have more solubility in oil than solid lipids[8,9].

NLCs have higher loading capacity and controlled drug released due to the dissolution of the drug in the oil and encapsulation in solid lipid phase[3].

1.1.3. Lipid drug conjugates

SLNs and NLCs can incorporate lipophilic drugs with a high efficiency or hydrophilic drugs at low concentrations due to partitioning effects during the processes. Lipid drug conjugates overcome this problem with a drug loading capacity of up to 33%. LDCs are prepared by salt formation (e.g. with a fatty acid) or by covalent linking (e.g. to esters or ethers). In salt formation, the free drug base and fatty acid are dissolved in an adequate solvent and then the solvent is evaporated under reduced pressure. The selected drug should have an amino or hydroxyl group as the functional groups which can be conjugated with the carboxyl group present in the fatty acid[10]. For the covalent linking of the drug salt and a fatty alcohol react in presence of a catalyst and the resulting product is then purified by recrystallization. The obtained LDC bulk is then processed with an aqueous surfactant solution to a nanoparticle formulation using high pressure homogenisation[2].

1.2. Preparation techniques of lipid nanoparticles

Different techniques can be used for SLNs and NLCs production, such as high-pressure homogenization, emulsification-sonication, microemulsion, solvent emulsification-evaporation, solvent diffusion, solvent injection, and double emulsion. Among them, high pressure homogenization and microemulsion have demonstrated a strong potential for scale up in industrial production[4,6]. Microemulsion and emulsification-sonication are described below. Other techniques are summarized in table 1.

Table 1: Techniques for nanoparticle preparation. Adapted from[4].

Method of preparation	Principle	Authors	Ref
High pressure homogenization	Lipids are melted at a temperature 5-10ºC above the melting point and the drug is dissolved in melted lipids. Hot homogenization: A hot aqueous surfactant is added and homogeneously dispersed by a high shear mixing device and this hot pre-emulsion is subjected to a high-pressure homogenizer. The resulting nanoemulsion is then cooled down to room temperature. Cold homogenization: The solidification of the drug-loaded lipid is carried out in liquid nitrogen followed by gridding in a powder mill and dispersing the powder in an aqueous surfactant dispersion medium and subjected to a high-pressure homogenizer.	Schwarz et al. (1994)	11
Solvent Emulsification-Evaporation	Lipophilic material is dissolved in a water-immiscible organic solvent that is emulsified in an aqueous phase. Upon evaporation of the solvent under reduced pressure, a nanoparticle dispersion is formed by precipitation of the lipid in the aqueous medium.	Sjöström and Bergenståhl (1992)	12
Solvent diffusion	Organic solvents are mutually saturated with water to ensure initial thermodynamic equilibrium of both liquids. The emulsion is then passed into water under continuous stirring, which leads to solidification of dispersed phase forming lipid nanoparticles.	Trotta et al. (2002)	13
Solvent injection	Lipids are dissolved in a water-miscible solvent or water and quickly injected into an aqueous solution of surfactant through an injection needle.	Schubert et al. (2003)	14
Double emulsion	Based on solvent emulsification-evaporation method. Drug and stabilizer are encapsulated in the inner aqueous phase of the water-in-oil-in-water (w/o/w) double emulsion. Stabilizer prevents the drug partitioning to the other aqueous phase during solvent evaporation.	Cortesia et al. (2002)	15

1.2.1. Microemulsion technique

The microemulsion technique was developed by Gasco in 1997 and it is based on the dilution of microemulsions[16,17]. Microemulsions are two-phase systems composed of an inner and outer phase, such as o/w microemulsion. They are produced by stirring mixture at 65º-70ºC which is typically composed of low melting fatty acids, an emulsifier, co-emulsifier and water. The hot emulsion is then dispersed in cold water under stirring. Typical volume ratios of the hot microemulsion to cold water are in the range of 1:25 to 1:50. Excess of water needs to be removed by ultrafiltration or lyophilisation to obtain a concentrate dispersion. Disadvantages of this method include the need of high concentrations of surfactants and co-surfactants[4].

Later, in 2006, Mumper and Jay patented a microemulsion-based method to produce SLNs and NLCs[18]. In this technique, an emulsifying wax is melted (37-55ºC) and water is then added at the same temperature under minimal stirring to form a homogeneous solution. Upon the addition of surfactant in water a clear and stable liquid matrix o/w microemulsion is formed. Nanoparticles are precipitated from this microemulsion by cooling of the undiluted microemulsion to room temperature or to 4ºC. An

advantage of this technique is that it can be formulated at mild operating temperatures, rapidly, reproducibly and cost-effectively in a one-step process and confined to a manufacturing vessel, vial or container. All ingredients are biocompatible, well-defined and uniform nanoparticles (50 to 300 nm) can be reproducibly obtained with no need of organic solvents during the preparation and with very high entrapment efficiencies, especially for water insoluble drugs[19,20].

1.2.2. Emulsification-sonication

Lipids are melted at 5-10ºC temperature above the melting point and the drug is dissolved/dispersed in the melted lipids. A hot aqueous surfactant is added to the drug. Melted lipids are homogeneously dispersed by a high shear mixing device and then sonicated and cooled to room temperature to allow the formation of solid lipid nanoparticle[21,1].

It is believed that ultrasonic emulsification happens through two mechanisms. First is the application of an acoustic field that produces interfacial waves which become unstable and resulting in the eruption of the oil phase into the water medium in the form of droplet (Figure 4-A). Second, the application of low frequency ultrasound causes acoustic cavitation, that is, the formation of bubbles by the pressure fluctuations of a simple sound wave. Each bubble collapse event causes extreme levels of highly localised turbulence. The turbulent micro-implosions act as a very effective method of breaking up primary droplets of dispersed oil into smaller droplets (Figure 4-B)[22].
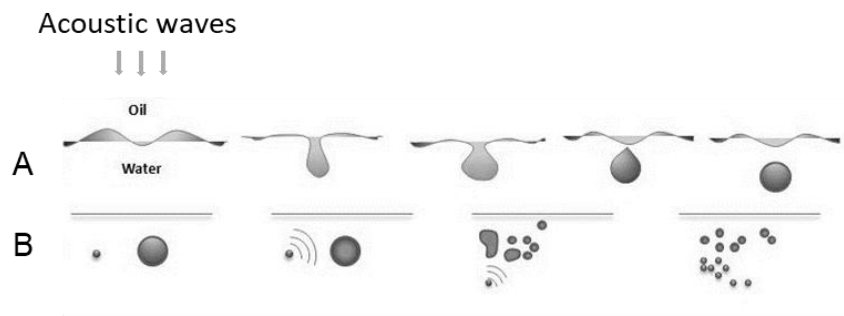
Figure 4: Ultrasound emulsification: droplet formation and break-up. Adapted from[23].

1.3. Influence of nanoparticle formulation
1.3.1. Influence of lipid composition

Lipid composition affect the average particle size of lipid nanoparticles. Size of nanoparticles increase with lipids with higher melting points due to the higher viscosity of the dispersed phase. There are other critical parameters for nanoparticle formation such as velocity of lipid crystallization, lipid hydrophilicity (influence on self-emulsifying properties) and the shape of the lipid crystals and consequently the surface area[17].

1.3.2. Influence of emulsifier

The choice of the emulsifiers (known as surfactant) and their concentration have an impact on the quality of the particle dispersion. Higher concentrations of emulsifier reduce the surface tension and facilitate the particle partition during homogenization. The decrease in particle size is related with the increase in surface area. The process of a primary coverage of the new surfaces competes with the agglomeration of uncovered lipid surfaces. The primary dispersion must contain excessive emulsifier molecules, which should rapidly cover the new surfaces[6].

Surfactants are molecules that have polar and nonpolar domains and can be used for emulsion stabilization due to their property of self-aggregation in solution. Due to the simultaneous presence of lipophilic and hydrophilic parts in their chemical structure, surfactant concentration influences the micellar formation. Depending on the charge of the head group, conventional surfactants can be nonionic, cationic, anionic or zwitterionic[24].

1.3.2.1. Critical micelle concentration

A surfactant forms micelles in an aqueous solution when the amount exceeds a certain level known as the critical micelle concentration (CMC). There is an abrupt change in the physicochemical properties of a surfactant solution when the CMC is exceeded, for example, surface tension, electrical conductivity, turbidity and osmotic pressure due to different properties of surfactant molecules dispersed as monomers compared to micelles. Consequently, the surface tension of a solution decreases with increasing surfactant concentration below the CMC. The CMC of a surfactant solution depends on the chemical structure of the surfactant molecules, as well as on the solution composition. The CMC tends to decrease as the hydrophobicity of surfactant molecule increase or their hydrophilicity decreases. For ionic surfactants, CMC decreases considerably with increasing ionic strength, since counter ions screen the electrostatic repulsion between the charged head groups, reducing the magnitude of this unfavourable contribution to micelle formation[25].

1.3.2.2. Hydrophile-lipophile balance

The hydrophile-lipophile balance (HLB) is widely used to classifying surfactants and gives an indicator of their relative affinity for the oil and aqueous phase. High HLB number means that a certain molecule has a high ratio of hydrophilic groups to lipophilic groups and low values mean the opposite[25].

The HLB number of a surfactant gives an indication of its solubility in either the oil and/or water phases. Surfactants with a low HLB number (3-6) are predominantly hydrophobic, dissolve preferentially in oil, stabilize w/o emulsions, and form reverse micelles in oil. A surfactant with a high HLB number (10-18) is predominantly hydrophilic, dissolves preferentially in water, stabilizes the o/w emulsion, and forms micelles in water. A surfactant with an intermediate HBL (7-9) has no preference for either oil or water and is considered a good "weeting agent". Molecules with HBL numbers bellow 3 (very hydrophobic) and above 18 (very hydrophilic) are often not particularly surface active since they tend to accumulate preferentially in bulk oil or bulk water, rather than at an o/w interface. Emulsion droplets tend to coalescence when they are stabilizing by surfactants that have extreme or intermediate HLB.

Disadvantages of the HBL concept is that it does not take into account the fact that the functional properties of a surfactant molecule are altered significantly by changes in temperature or solution conditions[25].

1.4. Characterization of lipid nanoparticles

Characterization of lipid nanoparticles is crucial for its quality control. However, this is a challenge due to the complexity of the system and the colloidal size of the nanoparticles. Some of the parameters that are usually evaluated include particle size, zeta potential, degree of crystallinity, drug content and surface morphology[7].

1.4.1. Particle size and zeta potential

Photon correlation spectroscopy (PCS) and laser diffraction (LD) are the most used techniques to measure particle size. LD is based on the dependence of the diffraction angle on the particle radius, where smaller particles lead to more intense scattering at high angles than the larger particles, thus, this technique is most adequate for large particles (up to 3 μm)[4,26].

PCS also known as dynamic light scattering, measures the fluctuation of the intensity of the scattered light which is caused by particle movement. This method is a good tool for particle size measurement but is not able to detect large nanoparticles since it covers a size range from a few nanometres to 3 microns. Particles suspended in a liquid are constantly moving due to Brownian motion (movement of particles due to the random collision with molecules of the liquid that surrounds the particle). Small particles move quickly, while large particles move slower[4,26].

The polydispersity index (PdI) measures the size distribution of the nanoparticles, meaning that the lower the PdI value, the more monodispersed the nanoparticles are. PdI values below than 0.3 are considered as optimum values[4,26].

The zeta potential (ZP) indicates the overall charge that a particle acquires in a specific medium. Most liquids contain ions that can be negatively or positively charged and when a charged particle is suspended in a liquid, ions of an opposite charge will be attracted to the surface of the suspended particle. Ions close to the surface of the particle will be strongly bound, while ions that are far away will be loosely bound, forming what is called a diffuse layer (Figure 5) where a notional boundary lays any ions within this boundary will move with the particle when it moves in the liquid and any ions outside the boundary will stay where they are. The potential that exists between the particle surface and the dispersing liquid which varies according to the distance from the particle surface is the zeta potential. Therefore, the most important factor that affects zeta potential is pH[26].

This potential is measured using a combination of techniques such as electrophoresis and laser doppler velocimetry where it is measured how fast a particle moves in a liquid when an electrical field is applied[26].
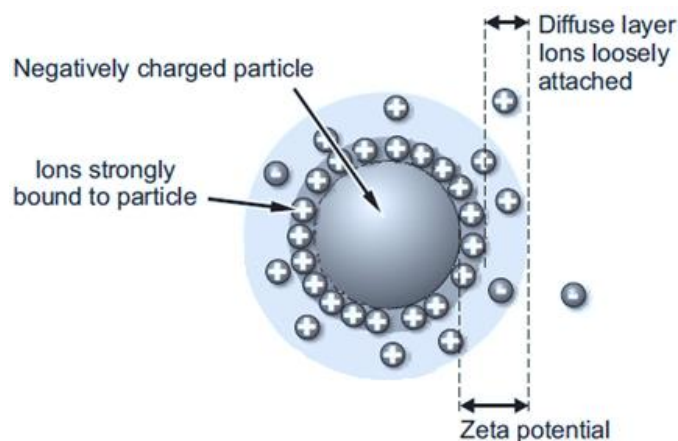
Figure 5: Representation of zeta potential in a nanoparticle. Adapted from[26].

The stability of the nanodispersion can be predicted from the zeta potential due to degree of repulsion between close and similarly charged nanoparticles in the dispersion. High ZP values (negative or positive) can predict the prevention of aggregation of the nanoparticles due to electric repulsion. On the other hand, low values of ZP can predict attraction of the nanoparticles where they can nanoparticles can flocculate or coagulate[26]. Both PdI and ZP can be measured by PCS[4]. Generally, nanoparticles more positive than +30mV or more negative than -30mV are considered stable[26].

1.4.2. Shape and morphology

Scanning electron microscopy (SEM), transmission electron microscopy (TEM) and atomic force microscopy (AFM) are the most usual techniques for determination of shape and morphology of lipid nanoparticles, although they can also be used for particle size and distribution studies. Opposite to the PCS and LD, SEM and TEM provide direct information of shape, morphology and size. SEM allows the observation of the sample after drying and coating with a thin layer of gold or platinum, allowing a resolution between 3 and 5 nm. TEM allows the observation of the sample after the deposition of a nanosuspension drop in a carbon covered copper grid dried at room temperature. AFM provides a tree-dimensional surface unlike SEM and TEM, being more appropriate for surface analysis. AFM also provides structural, mechanical, functional and topographical information about surfaces with nanometre to angstrom-scale resolution. This technique utilizes the force acting between a surface and a probing tip resulting in a special resolution of up to 0.01 nm for imaging[4,6,27].

1.4.3. Crystallinity and polymorphism

Characterization of the degree of lipid crystallinity and the modification of the lipid is critical due to correlation of these parameters with drug incorporation and release. In addition, the lipid matrix as well as the incorporated drug can undergo a polymorphic transition leading to a possible drug expulsion during storage[17].

Differential scanning calorimetry (DSC) and X-ray diffractometry (XRD) are widely used to investigate the status of the lipids. DSC uses the fact that different lipid modifications possess different melting

points and melting enthalpies, while XRD can identify specific crystalline compounds based on their crystal structure[17].

DSC is designed to measure heat exchanges during controlled temperature programs. Although DSC can monitor and quantify even minute thermal events in the sample and to identify the temperatures at which these events occur, it is a technique which does not directly reveal the cause of a thermal event. In common DSC investigations, the respective sample is heated or cooled at a controlled rate and the heat flow into or out of the sample is monitored in a quantitative way[28].

1.4.4. Encapsulation efficiency and drug loading

Encapsulation efficiency (EE) is defined as the ratio of encapsulated drug in nanoparticles to whole drug first incorporated in the lipid phase of NLC, multiplied by 100. This ratio can be calculated after quantification of the free and encapsulated fractions of the drug. The unencapsulated free drug may crystalize and/or dissolve in the aqueous phase. The crystalized fractions is usually micron in size, precipitates in the NLC system and can be removed by microfiltration or mild centrifugation. The aqueous phase can be separated from the nanoparticle by ultrafiltration, ultracentrifugation or size exclusion chromatography and the amount of dissolved or encapsulated drug can be quantified. Separated nanoparticles may be washed with water to remove the free drug absorbed on their surface. Dissolved drug also can be removed from aqueous phase with solvent extraction[3]. Quantification of free drug can be performed using high-performance liquid chromatography (HPLC). Drug loading (DL) is defined as the ratio of encapsulated drug to the amount of lipid phase or lipid nanoparticles in the NLC formulation, multiplied by 100[3].

1.4.5. Drug release

Release profiles are often biphasic where an initial burst release is followed by a prolonged release. The burst release usually occurs when hot homogenisation is used and very high temperatures are applied. The extent of burst release also depends on the amount of surfactant used. High surfactant concentration leads to high burst release and vice-versa. The higher the solubility of the drug in water phase the higher the burst effect. The solubility increases when increased temperature and increased surfactant concentrations are used. Consequently, when low production temperatures and low surfactant concentrations are used, little or no burst effect is observed[8,29].

Release kinetics depend on the release conditions and procedures. These procedures include filtration, centrifugation or dialysis, therefore, it is not easy to compare the results from distinct methods[17].

1.5. Sterilization of lipid nanoparticles

For the different routes of administration nanoparticles should be sterile. Sterilization should not modify the properties of nanoparticles and some of current techniques are aseptic production, filtration,

ɣ-radiation and autoclaving. Filtration is only possible if the mean particle size is below 200nm due to the quick block of filters. In the process of ɣ-radiation some free radicals are formed due to the high energy of the ɣ-rays, being able to react with sample components, leading to chemical modification and reduction of the physical stability of the nanoparticles. Autoclaving is commonly used but it is only possible if molecules are thermo-resistant[11,17].

1.6.   Storage of lipid nanoparticles

Storage stability involves chemical and physical aspects and includes the prevention of degradation reactions such as hydrolysis and maintenance of the initial particle size. It is required that SLN and NLC ingredients are chemically stable and nanoparticles have a very narrow size distribution to avoid crystal growth. Nanoparticles should also be resistant to temperature changes[17]. Lyophilisation and spray drying are good examples of techniques used for storage of lipid nanoparticles.

Lyophilisation is a promising way to increase chemical and physical stability over extended periods of time avoiding hydrolysis and Ostwald ripening. Ostwald ripening, also known as coarsening, consists in a decrease in total interfacial area due to decrease of the total energy of the two-phase system via an increase in the size scale of the second phase[30].

The first transformation of lipid nanoparticle lyophilisation is the passage from aqueous dispersion to powder that involves the freezing of the sample and the sublimation of water under vacuum. Freezing of the sample might cause stability problems due to the freezing out effect which results in changes of the osmolality and the pH. The second transformation is the re-solubilization that involves situations which favour particle aggregation, low water and high particle content and high osmotic pressure. The protective effect of the surfactant can be compromised and lipid content should not exceed 5%. The addition of cryoprotectants (place holders which prevent the contact between lipid nanoparticles) on the quality of the lyophilizates is essential due to decrease of osmotic activity of water and crystallization, favouring the glassy state of the frozen sample. Examples of cryoprotectants generally used are sorbitol, mannose, trehalose, glucose and polyvinylpyrrolidone[17].

Spray drying is an alternative procedure to lyophilisation, transforming an aqueous dispersion into a dry product. This method is cheaper comparing to lyophilisation. This technique converts a liquid into a dry system in a one-step process and can produce fine, dust-free powders as well as agglomerated ones, to precise specifications. In general, the process consists of four steps: atomization of the feed into a spray, spray-air contact, drying of the spray and separation of the dried product from the drying gas. Spray drying may cause particle aggregation due to high temperatures, shear forces and partial melting of the nanoparticles. Lipids with melting points above 70ºC are recommended[17,31].

1.7.   Lipid nanoparticles as oral drug delivery systems

Delivery of a drug molecule to a specific organ site is one of the most challenging research areas in pharmaceutical sciences. The development of a colloidal delivery system such as nanoparticles allowed the improvement of drug delivery. Nanoparticles as previous mentioned have some special

characteristics such as small size (10-1000 nm) and large surface area. Generally, the drug or a biological active material are dissolved, entrapped, adsorbed or attached. The advantages of nanoparticles as drug delivery systems rely on their biodegradability, non-toxicity and capability of being stored over long periods[6].

In the present work, the two antibiotics that will be used for encapsulation in lipid nanoparticles are ciprofloxacin and tobramycin, which are presently used in cystic fibrosis therapy. There are some studies of the encapsulation of these drugs in various types of lipid nanoparticles. Table 2 summarizes some of studies carried out for encapsulation of ciprofloxacin and tobramycin in both SLNs and NLCs.

Oral administration is the most preferred route for drug administration due to greater convenience, less pain, high patient compliance, reduced risk of cross-infection, and needle stick injuries[4].

The aim of oral administration is the improvement of oral bioavailability either by increasing gastrointestinal absorption or by bypassing the first-pass metabolism[4].

Table 2: Previous studies of encapsulation of ciprofloxacin and tobramycin in SLNs and NLCs.

Antibiotic	Type of nanoparticle	Formulation	Method	Application	Year	Ref
Ciprofloxacin	SLN	Stearic acid, phosphatidylcoline, sodium taurocholate	Microemulsion using high-speed homogenizer	Systemic delivery	2008	32
	SLN	Cholesterol, Tween 80, ethanol, acetone	Solvent emulsification/ evaporation and sonication	Ocular delivery	2011	33
	SLN	acetyl palmitate, PEG 100 glyceryl stearate, glyceryl trimyristate, monoglycerides and diglycerides of stereate	Solvent diffusion	Ocular delivery	2012	34
	SLN	Softisan 154, Dynasan 118, Imwitor 900, stearic acid, Tween 80 and sodium deoxycholate	ultrasonic melt-emulsification	-	2017	35
Tobramycin	SLN	Stearic acid, epikuron 200, taurocholate	Microemulsion under mechanical stirring	Duodenal delivery	2000	36
	SLN	Stearic acid, epikuron 200, taurocholate	Microemulsion under mechanical stirring	Ocular delivery	2002	37
	NLC	Precirol® ATO 5, Compritol® 888 ATO, Miglyol® 812, Tween 80, Poloxamer	Hot melt homogenization technique	Pulmonary delivery	2016	38

1.7.1. Ciprofloxacin

Ciprofloxacin (figure 6) is a broad-spectrum fluoroquinolone antibiotic. The compound has a high activity against Gram-positive and Gram-negative bacteria, however is more active against Gram-negative bacteria, such as *Pseudomonas aeruginosa*. Ciprofloxacin inhibits bacterial DNA gyrase, an enzyme essential for DNA replication[32,39,40]. Some of its physical and chemical properties are listed in table 3.
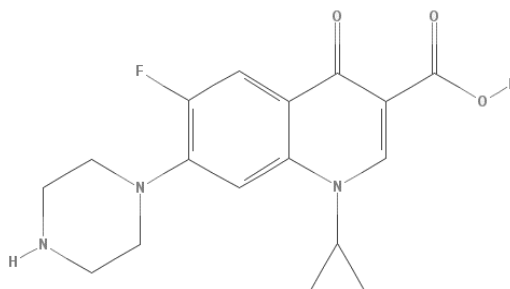
Figure 6: Molecular structure of ciprofloxacin. Adapted from[40].

Table 3: Physical and chemical properties of ciprofloxacin. Data obtained from[40].

Properties	Value
Molecular weight (g/mol)	331.347
pH	acid
pKa	6.09 (carboxylic acid group) 8.74 (nitrogen on piperazinyl ring)
log Kow	0.28
Melting point	225-257ºC

1.7.2. Tobramycin

Tobramycin (figure 7) is an amiglycoside antibiotic. The molecule is active against gram negative bacteria, especially *Pseudomonas* species. Tobramycin binds irreversible to a specific aminoglycoside receptor on the bacterial 30S small ribosomal subunit, interfering with the initiation complex between messenger RNA and the ribosomal subunit. This leads to an inhibition of protein synthesis initiation, leading to bacterial cell death. Tobramycin also induces misreading of the mRNA template, causing incorrect amino acids to be incorporated in the polypeptide chain during the elongation process[41]. Some of its physical and chemical properties are listed in table 4.
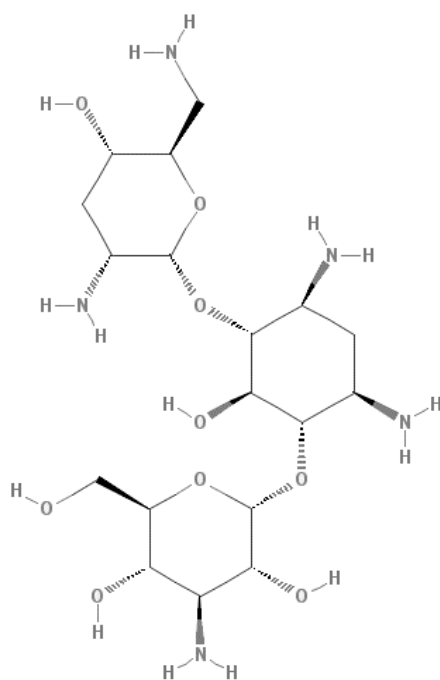
Figure 7: Molecular structure of tobramycin. Adapted from[41].

Table 4: Physical and chemical properties of tobramycin. Data obtained from[41].

Properties	Value
Molecular weight (g/mol)	467.52
pH	basic
pKb	pKb1 = 8.6 pKb2 = 8.8 pKb3 = 9.0
log Kow	-5.8
Melting Point	168 -178ºC

1.8. Cystic fibrosis disease

Cystic fibrosis is an autosomal recessive disorder that affects approximately 70 000 individuals worldwide[42,43]. In Portugal the incidence of CF is estimated to be about 1:6000[44]. .

CF results from the inheritance of mutant alleles of the gene encoding the cystic fibrosis transmembrane conductance regulator (CFTR) from each parent. The gene was first identified and isolate by Rommens J. and colleagues in 1989[45].

CFTR is largely expressed in the apical membranes of epithelial cells of organs and glands such as sweat, pancreas, gastrointestinal, reproductive tracts and submucosal glands and airway epithelia, that line the cylindrical structures of tissues that secrete fluids often rich in mucus and other proteins. The airways are among the tissues with the highest expression of CFTR. Mutations in the gene are accompanied by a reduction or even a total absence of CFTR activity at the cell surface, causing deficient cAMP-dependent chloride and bicarbonate secretion in the airways[46].

CF patients who carry a single CFTR mutation may retain 50% of CFTR activity but are unaffected. Patients carrying two mutant CFTR alleles in which one mutation retains residual CFTR function have

less aggressive disease phenotypes and better overall survival than those who carry severe mutations in both alleles[46].

CF individuals have viscous secretions in the airways of the lungs and in the pancreas vessels, which cause obstruction and lead to inflammation, tissue damage and destruction of both organ systems. Other organ systems containing epithelia such as sweat glands, biliary duct of the liver, male reproductive tract and intestine, are also affected. Loss of pancreatic exocrine function results in malnutrition and poor growth, and diet supplements are usually prescribed to the CF patient[42].

The airway surface liquid and mucus layer is a complex and dynamic structure that is continuously changing in response to signals from the environment and the host. Major functions include the clearance of pathogens and to provide a protective barrier against toxic endogenous and exogenous products. CFTR plays an important role in providing water to balance the hydration in airways compartment by secreting chloride and regulating sodium absorption. The CFTR mutation results in changes in osmotic pressures and electro-neutrality, leading to an excessive sodium and water absorption. These events culminate in a chronic retention of pathogens and a secondary inflammatory response[47].

1.8.1. Opportunistic pathogens in cystic fibrosis disease

CF airways are not infected at birth and bacterial opportunists enter the upper and lower respiratory tract by inhalation or aspiration. These bacteria growth and establish themselves in the lungs, leading to a local inflammation and the establishment of a chronical inflammatory response. This triad of chronic obstruction, infection and inflammation leads to a lifelong degradation of the lung anatomy and function, contributing to the premature death of persons with CF. Respiratory failure caused by infection and inflammation is the cause of about 80% of mortality among CF patients[46,48].

The bacteria most commonly believed to be pathogenic in CF include *Pseudomonas aeruginosa, Staphylococcus aureus, Hemophilus influenza, Stenotrophomonas maltophilia, Achromobacter xylosoxidans* and *Burkholderia* species[48].

1.8.1.1. *Burkholderia cepacia* complex

The *Burkholderia cepacia* complex (Bcc) is a heterogeneous group of gram-negative comprising at least 20 genetically related bacterial species. These bacteria were initially described as plant pathogens in the 1950s, being the causative agent of soft onion rot[49,50]. These bacteria are important opportunistic pathogens, especially in cystic fibrosis patients, and are associated with a worse prognosis and decreased life expectancy. One of the most striking features of Bcc infections is the unpredictable clinical outcome, ranging from asymptomatic carriage to the cepacia syndrome. The large majority of CF patients infected with Bcc develop a chronic infection that can last for years, leading to progressive loss of lung function[51]. Several Bcc species have been shown to be transmissible from one CF patient to another. *B. cenocepacia* and *B. multivorans* are predominant in CF[50].

1.8.2. Current antibiotic therapies of cystic fibrosis patients

CF individuals are highly susceptible to bacterial respiratory infections, thus intensive antibiotic therapy is in use to maintain lung function and reduce inflammation in infected patients[48].The eradication of infections caused by bacteria is very difficult and often unpredictable, due to their intrinsic resistance to the vast majority of clinically available antimicrobials[52]. The correct choice of the antimicrobial to be used involves the characterization of susceptibility profiles of the bacteria. Current therapies use combinations of two or three antibiotics[52]. For treatment of chronic *P.aeruginosa* other strategies have emerged such as the use of aerosolized antibiotics. Some examples are tobramycin inhalation solution (TIS) and Bramitob®. Tobramycin has also been developed as an inhalation dry powder (TOBI® Podhaler®). Other aerosolized antibiotics have been used such as aztreonam lysine (Cayston®) and colistin (Colobreathe®). There are several antimicrobials in development such as liposomal amikacin, ciprofloxacin dry powder, levoxacin inhalation solution and new combinations of antibiotics[48].

Examples of current antibiotic treatment for other bacterial pathogens such as *Burkholderia cepacia* complex are Doxycyclin for oral administration and Meropenem and Tobramycin for intravenous administration[48].

1.9.   Lipid nanoparticle-bacteria interaction

There are multiple bacterial barriers that decrease antibiotics efficacy. Some of those barriers are bacterial biofilms, cell walls and destructive enzymes. In the case of cystic fibrosis, the viscous mucus that is produced in the airways represents an additional barrier to antibiotics penetration. Usually antibiotics are ineffective against biofilms due to their inability to cross the matrix. This matrix is composed of polysaccharides, proteins, glycoproteins and glycolipids and in some cases extracellular DNA. The bacterial cell wall is another obstacle due to its electrical charge (both gram-negative and gram-positive are negatively charged). The enzymatic barrier is composed by several enzymes produced by bacteria that can affect the antibiotics[53]. Nanoparticles are a solution that can overcome some of these problems. Nanoparticles can help in bypass bacterial drug resistance acting on the alteration of bacteria efflux pump activity, antibiofilm activity, enhanced penetration through biofilms, protection against enzymatic degradation, specific targeting and sustained-release. Some factors that can affect this interaction is the size, surface hydrophobicity and zeta potential of nanoparticles[53].

1.10.   *C. elegans* as an animal model of infection

Caenorhabditis elegans is a small (approximately 1 mm, in adulthood), free-living soil hermaphroditic nematode, that feeds on microbes. The nematode is a widely used model due to the ability to grow hundreds of animals on a single Petri dish (each adult can lay between 250 and 300 eggs), feeding on bacteria (usually *Escherichia coli*), small size, transparency, rapid life cycle, short lifespan (2-3 weeks), easy and inexpensive growth in the laboratory[54,55]. The nematode grow at temperatures up to 25 °C and can be vortexed, centrifuged, and frozen[56]. The worm can be easily maintained in the laboratory, where it grows on agar plates or liquid cultures with *E. coli* as food source. The nematode is an important model

system for many biological research fields such as genetic, genomics, cell biology, neuroscience and ageing. There is a high conservation of genome sequences between the worms and vertebrates (genome of *C. elegans* has approximately 72% similarity to humans). However, this model have some limitations because it lacks some specific tissues such as bones, eyes, ears and circulatory system[54,55,57]. The life cycle of the animal (figure 8) comprises the embryonic stage, four larval stages (L1-L4) and adulthood.
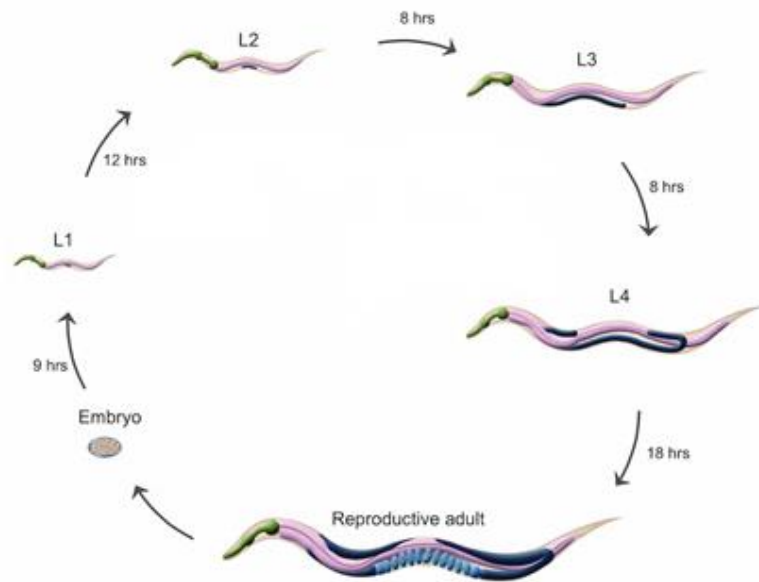
Figure 8: Representative stages of the *Caenorhabditis elegans* life cycle (L1 through L4). L4 larvae molt into young adults which then develop into reproductive adults that survive for approximately 3 weeks under normal laboratory conditions. Adapted from[58].

Feeding of *C. elegans* involves food ingestion, digestion, nutrient absorption and defecation. Worm is a filter feeder: it draws bacteria suspended in liquid into its pharynx, traps the bacteria, and ejects the liquid. Two motions are involved in the feeding behaviour of *C. elegans*: pharyngeal pumping and isthmus peristalsis. Pumping is a contraction-relaxation cycle in which nanoparticles and liquid are sucked in. During relaxation, liquid is ejected to the exterior and bacteria are retained in the pharynx and transported into the intestine. *C. elegans* digestion seems to start with passage of bacteria through the grinder, which damages the bacterial cells. Next, the bacterial cell wall and the plasma membrane are degraded by secreted lysozymes and saposins/amoebapores in the intestine, and the contents of the bacteria pass to the intestinal lumen. Hydrolysis of the macromolecules is performed by secreted peptidases and lipases in the anterior gut. Finally, the absorption of nutrients mostly occurs in the apical part of the intestinal cells owing to the presence of microvilli, which increase the surface area of contact between the cell and the intestinal lumen, and also contains peptide transporters and nucleoside transporters, among others that are involved in absorption[54].

1.10.1. *C. elegans* as a bacterial Infection model

As the worm feeds mainly of *E. coli*, the food source can be replaced by the pathogen under study and following the disease progress. Several strains of pathogens have been tested in *C. elegans*. Some pathogens produce lethal toxins and kill the nematode while others are virulent by provoking intestinal

infections and signs of illness such as locomotion defects, distended intestine, paralysis or erratic movement. The nematode has been used for to study Gram-positive human pathogens such as *Staphylococcus aureus* and Gram-negative such as *Pseudomonas aeruginosa* and strains belonging to Bcc species isolated from CF[55,56].

1.10.2. *C. elegans* as a tool for *in vivo* nanoparticle assessment

The main path of uptake of nanoparticles in *C. elegans* is the alimentary system where the worms ingest nanoparticles actively during feeding or passively diffuse through the cuticle during exposure or the vulva, anus, and excretory pore, because these openings connect the body of the worm to its environment[54].

The particle size should be smaller than 1000nm to be ingested, that is the dimensions of the nematode mouth. This ingestion could occur through two different mechanisms: voluntary ingestion, or non-voluntary ingestion of the nanoparticles simultaneously with ingestion *of E. coli* OP50 bacteria due to continuous pumping action of the pharynx[57].

1.11. Objetives

The first aim of this work was the development, optimization and characterization of a nanostructured lipid carrier. Different fatty acids (lauric acid-C12, myristic acid-C14, palmitic acid-C16 and stearic acidC-18), oils (coconut oil and sunflower oil) and surfactants (Tween 80 and Span 80) were used (Table 5). Second objective of this work was the encapsulation of two antibiotics, ciprofloxacin and tobramycin, which are currently used in CF therapy[48]. Nanoparticles were characterized by dynamic light scattering (to determine the average size, polydispersity index and zeta potential), differential scanning calorimetry, encapsulation efficiency, drug loading capacity and release profile.

Nanoparticles with encapsulated ciprofloxacin were fed to infected *C. elegans* as an animal model of infection. Pathogens belonging to the Bcc group (*Burkholderia contaminans* IST408 and *Burkholderia cepacia* K56-2) were used as model pathogens to infect the *C. elegans* nematode. As the worm feeds mainly of *E. coli*, the food source can be easily replaced by the pathogen under study following the disease progress. After the nematode infection, the efficacy of encapsulated antibiotics in nanoparticles can be assessed by comparing the survival of nematode in presence or absence of nanoparticles.
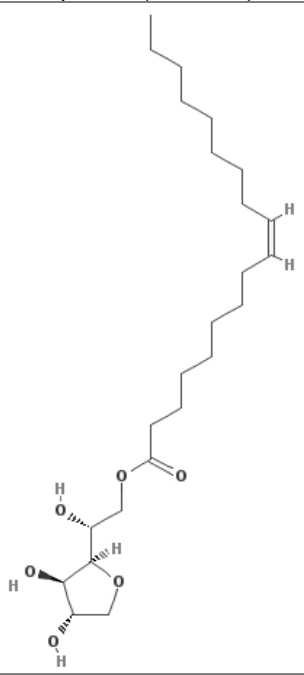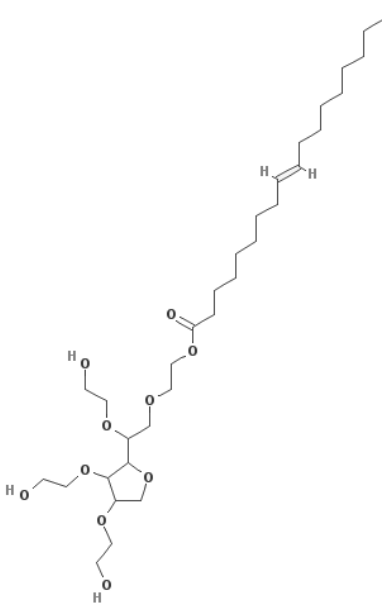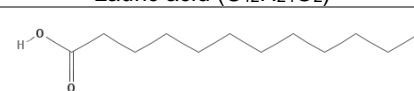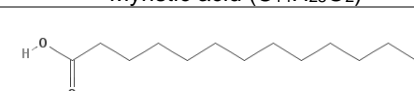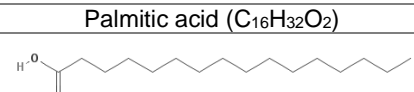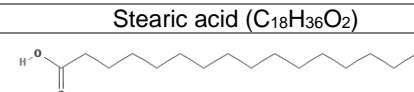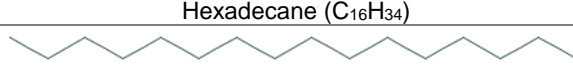
2.   Materials

Lipids used were lauric acid (≥99%) and palmitic acid purchased from Sigma-Aldrich Chemicals (St. Louis, MO, USA), myristic acid (99%), coconut oil and stearic acid from Acros Organics (Belgium). Sunflower oil is a commercial alimentary product and were purchase from Fula (Portugal). Surfactants were Tween 80 (Merck-Schuchardt, Germany) and Sorbitan monoleate (Thermo Fisher Scientific, USA). Co-surfactant was Hexadecane (≥99%) from Sigma-Aldrich (St. Louis, MO, USA). Tobramycin, Ciprofloxacin and Fluorescamine were purchased from Sigma-Aldrich Chemicals (St. Louis, MO, USA). DiOC18(3) were purchased from invitrogen by Thermo Fisher Scientific (Carlsbad, California, USA).

Water was from a Millipore Milli-Q® ultrapure water purification unit.

Table 5: Structure of surfactants (Tween 80 and Span 80), fatty acids (lauric acid, myristic acid, palmitic acid and stearic acid) and co-surfactant hexadecane.

	Structure	
	Span 80 ($C_{24}H_{44}O_6$)	Tween 80 ($C_{32}H_{60}O_{10}$)
Surfactant	Ref 59	Ref 60
Fatty acid	Lauric acid ($C_{12}H_{24}O_2$) Ref 61	Myristic acid ($C_{14}H_{28}O_2$) Ref 62
	Palmitic acid ($C_{16}H_{32}O_2$) Ref 63	Stearic acid ($C_{18}H_{36}O_2$) Ref 64
Co-surfactant	Hexadecane ($C_{16}H_{34}$) Ref 65	

3.   Nematode and bacterial strains

Caernorhabditis elegans (strain Bristol N2) was obtained from Caernorhabditis Genetics Center - University of Minnesota, Minneapolis, USA.

E. coli OP50 (uracil-requiring mutant of *E. coli*) was obtained from Medical Research Council Laboratory of Molecular Biology, Hills Road, Cambridge, England[66].

B. contaminans isolate IST408 were obtained from bronchial secretions of a patient with CF in January 1995 from the HSM CF Center, Lisbon, Portugal[67,51].

B. cenocepacia K56-2 was obtained from the sputa of CF patient from Hospital for Sick Children, Toronto, Ontario, Canada[68].

4.   Methods

4.1.   Preparation of lipid nanoparticles

Two different methodologies were used for lipid nanoparticle production. In the first methodology nanostructured lipid carriers were prepared by a simple magnetic stirring method based on the microemulsion technique[18,25,69]. Both aqueous and lipid phases were separately prepared before mixing. The aqueous phase was composed of milli-Q water (90.7% w/w), Tween 80 (4.9% w/w) as a surfactant and hexadecane (1.6% w/w), as a co-surfactant. The lipid phase was composed of myristic acid (0.5% w/w), lauric acid (0.9 %w/w) and coconut oil (1.4 %w/w). The two phases were heated in a worm bath at 70°C under magnetic stirring for 15 minutes to fully melt lipids. Then the lipid phase was added to aqueous phase and heated for 1 hour under stirring at 70°C. After the heating step, samples were gradually cooled during 1h under stirring until were reached 20°C [69,70] (Formulation NLC_1).

In the second methodology, sonication was used instead of gradual cooling. After the heating step, samples were sonicated for 5 minutes (48% amplitude; pulse 10/5 seconds ON/OFF) in a probe-type sonicator Sonoplus (Bandelin, Germany). For this methodology, different lipids were used (lauric acid, myristic acid, palmitic acid and stearic acid) as well as different surfactants (Span 80 and Tween 80) and oils (sunflower oil and coconut oil) with the proportions of 0.8%w/w, 1%w/w and 1.2%w/w, respectively. Span 80 was added to the lipid phase instead of aqueous phase due to its high lipophilicity. For the loaded nanoparticles, the antibiotics ciprofloxacin and tobramycin were added to the aqueous phase 15 min before the mixing step (Formulation NLC_2 to NLC_CIP). The different formulations of lipid nanoparticles used in this study and respective composition are represented in table 6 (Formulation NLC_1 to NLC_CIP).

Table 6: Different formulations of lipid nanoparticles

Formulation		Aqueous phase	Lipid phase
NLC_1		Milli-Q water, hexadecane, Tween 80	Myristic acid, lauric acid, coconut oil
NLC_2		Milli-Q water	Span 80, coconut oil, stearic acid
NLC_3	Empty nanoparticles	Milli-Q water, Tween 80	sunflower oil, stearic acid
NLC_4			Span 80, sunflower oil, stearic acid
NLC_5		Milli-Q water	Span 80, sunflower oil, lauric acid
NLC_6			Span 80, sunflower oil, myristic acid
NLC_7			Span 80, sunflower oil, palmitic acid
NLC_TOB	Loaded nanoparticles	Milli-Q water, tobramycin	Span 80, sunflower oil, stearic acid
NLC_CIP		Milli-Q water, ciprofloxacin	

4.2. Characterization of lipid nanoparticles

4.2.1. Size and zeta potential

The mean particle size (in nm), polydispersity index and zeta potential (in mV) were determined by photon correlation spectroscopy in a Zetasizer Nano ZS (Malvern Instrument, Worcestershire, UK). Measurements of size and polydispersity index were made in glass cells at 25°C with dynamic light scattering detected at an angle of 173°. Volume of sample were 1mL.

Measurements of Zeta potential were performed in a folded capillary cell (DTS1070, Malvern, UK) at 25° and diluted 1:100 in milli-Q water. A set of triplicate measurements was performed for all samples.

Formulation NLC_4, NLC_CIP and NLC_TOB were stored at room temperature for 60 days and the size, PdI and ZP were measured after 1, 30 and 60 days upon preparation.

4.2.2. Microscopy observation

The morphological study of NLCs was performed by transmission electron microscopy (TEM) in a (Hiatchi H8100, Tokyo, Japan) with incorporated LaB6 filaments and a CCD camera (Olympus-Keenview), operated at an acceleration voltage of 200kV. For sample preparation, a drop of the nanoparticle suspension was deposited in a carbon covered copper grid and dried at room temperature. Samples analysed were NLC_1, NLC-4, NLC_CIP and NLC_TOB.

4.2.3. Differential scanning calorimetry

A 0.5 ml sample of nanoparticle suspension was dried in a VACUtherm (Thermo Scientific, USA) for 72h. DSC thermal analysis were obtained using DSC 200 F3 Maia® (Netzsch, Germany). For DSC analysis, 5 mg of dried nanoparticle were crimped in a standard aluminium pan and heated from 25ºC to 120ºC (for remove residual water) and then cooled to 25ºC under constant purging of nitrogen. This set of temperatures was repeated twice.

4.2.4. Washing of lipid nanoparticles by ultrafiltration

Lipid nanoparticles washing was performed by ultrafiltration using Spin-X® UF centrifugal filter device with a cut-off of 10,000 Da (Corning, USA). A 3 mL sample of the nanoparticle solution was added to the concentrator and then centrifuged at 5000 rpm during 15 min in a centrifuge (Labofuge 200, Heraeus Sepatech). The filtrate was collected and the sample remaining in the upper chamber was washed with water with a volume corresponding to the filtrate, and centrifuge once more. This step was performed tree times and the filtrate was collected for quantification of free drug.

4.2.5. Encapsulation efficiency and drug Loading

The encapsulation efficiency (EE) and drug loading capacity (DL) of antibiotic ciprofloxacin in NLCs were determined indirectly by measuring the concentration of free antibiotic in aqueous phase using reverse-phase high performance liquid chromatography (RP-HPLC).

Percentages of EE and DL were estimated according to equations 1 and 2, respectively.

$$EE\% = \frac{W_{total} - W_{free}}{W_{total}} \times 100$$

Equation 1

$$DL(\%) = \frac{W_{total} - W_{free}}{W_{lipid} + (W_{total} - W_{free})} \times 100$$

Equation 2

Where W_{total} is the total weight of drug added, W_{free} is the weight of free drug dissolved in dispersion medium, W_{lipid} is the total lipids weight in the formulation.

4.2.5.1. Tobramycin

The absence of chromophore or fluorophore groups in the tobramycin, makes direct UV or fluorometric detection inapplicable and chemical derivatization of primary amino groups is often carried out[71]. In this work, fluorescamine was used for derivatization of tobramycin for UV-VIS spectrophotometric and spectrofluorometric detection.

Supernatants obtained during the centrifugation in Spin-X®UF concentrator devices were analysed by UV-VIS spectrophotometer after derivatization with fluorescamine. Supernatant was diluted 1:2(v/v) in a fluorescamine solution at 0.5%(w/v) in ethanol and incubated at room temperature under agitation (100 rpm) protected from light for one hour before analysis. Absorbance of samples was measured at 390 nm using a U-2000 Hitachi Spectrophotometer (Japan) using a 0.1cm quartz cell[38,72,66]. The calibration curve obtained is shown in annex 1.

Supernatants obtained during the centrifugation in the Spin-X®UF concentrator devices were also analysed by fluorescence after derivatization with fluorescamine. Spectrofluorimetric detection enables

a more sensitive analysis than spectrophotometry. A fluorescamine solution was prepared at 1.5mg/mL in acetone. Aqueous borate buffer solution was prepared by dissolving 0.620g of boric acid and 0.750g of potassium chloride in 200ml of milli-Q water. The pH of the solution was adjusted with 0.1M sodium hydroxide solution. 150µL of supernatant was added 75µL of fluorescamine solution and 775µL of borate buffer[71]. After 5 minutes, the fluorescence intensities of the resulting solution were measured at 469 nm with excitation at 388 nm in a 0.1cm quartz cell in a Varian Cary eclipse fluorescence spectrophotometer. The calibration curve obtained is shown in annex 2.

4.2.5.2. Ciprofloxacin

Ciprofloxacin was quantified with RP-HPLC (reverse phase-high performance liquid chromatography. The HPLC system was composed of a L-7100 Pump (LabChrom, Hitachi, Merck, Japan) a UV-VIS detector (L-4000, Hitachi, LabChrom, Japan) and a C18 reversed-phase column Purospher® RP-18 (LioChroCart®, Merck Millipore, Germany) with the following dimensions: length 250 mm, inner diameter 4 mm and particle size 5 μm at room temperature. The HPLC method used was adapted from Wu, Shihn-Sheng, et al.[39], with slightly modifications. The isocratic mobile phase used was 88:12 (v/v) 2% aqueous solution of acetic acid – acetonitrile. The flow rate was fixed at 0.5 mL/min with an injection volume of 10 μL. Detector was set at 280 nm.

4.2.6.   Drug release

Preliminary release studies of ciprofloxacin from nanoparticles were performed using regenerated cellulose dialysis tubing (Orange scientific, Belgium) with a cut-off between 12,000 and 14,000 Da. A 5 ml nanoparticle sample suspension was added to the dialysis tubing for 45 mL of phosphate buffer (pH=7.4) at 37ºC, protected from the light and under stirring. 1 mL aliquot of the release medium was taken at t=0, t=30 min, t=1h-t=8h, t=10h, t=24h, t=36h, t=48h. Samples were analysed by high performed liquid chromatography. At the end of the experience the size (in nm) and PdI of the nanoparticle suspension was measured by DLS.

4.3.   Maintenance and cultivation of *C. elegans*

C. elegans can be maintained on NGM I plates with *E. coli* OP50 till three weeks at 20ºC. For the assays nematodes were transferred every 2 days on fresh NGM I plates containing *E. coli* OP50.

NGM I contained, per liter of distillate water, 3g NaCl, 2.5g tryptone, 17g agar, 5 mL of nystatin (10mg/mL in ethanol), 25 mL of 1M K_3PO_4 buffer (pH 6), 1 mL of 1M $CaCl_2$, 1 mL of 1M $MgSO_4$, 1 mL uracil (2mg/mL) and 0.5 mL cholesterol (10mg/mL in ethanol).

4.3.1. Preparation of *C. elegans* eggs

In order to synchronize cultures of *C. elegans*, a plate containing worms and eggs was washed four times with 1 mL of sterile water and the suspension was dispersed by three tubes. To the suspension, 500 μL of a hypochlorite solution (containing 600 μL of water, 500 μL sodium hypochlorite (12%) and 400 μL NaOH (6N), pH 6.0) were added and vortexed for approximately 5 minutes until all worms were dissolved. The suspension was centrifuged (1 minute, 3200 rpm), and the supernatant was carefully discarded. The pellet was washed with 1 mL of sterile water and centrifuged (1 minute, 3200 rpm). After washing, the supernatant was discarded and the pellet of the three tubes was resuspended with 100 μL of M9 buffer. This suspension was pipetted into a NGM I plate previously inoculated with *E. coli* OP50 and incubated at 20°C.

M9 buffer contained, per liter of distillate water, 3g KH_2PO_4, 6g Na_2HPO_4, 5g NaCl and 1 mL $MgSO_4$.

4.4. Toxicity assay in liquid medium

The evaluation of the toxicity of ciprofloxacin and tobramycin was assessed by quantifying the survival of the nematode *Caernorhabditis elegans* upon incubation in the presence of increasing concentrations of each antibiotic under study. In this work, the toxicity assays were performed in liquid media (supplemented K medium). The Supplemented K medium contained per liter 100 mL of K medium 10x concentrated, 25 mL of 1M K_3PO_4 buffer (pH 6), 1 mL of 1M $CaCl_2$, 1 mL of 1M $MgSO_4$ and 0.5 mL cholesterol (10mg/mL in ethanol). The K medium contained 53 mM NaCl and 32mM KCl.

The toxicity liquid assays were performed in a 96-well polystyrene microtiter plate (Greiner BioOne). In each experiment, three wells were used for each compound concentration (2, 4, 8, 12, 32, 64, 128, 256, 512 and 1024 μg/mL). These wells contained 90 μL of the supplemented K medium, 90 μL of each antibiotic and 20 μL of heat-killed *E. coli* OP50 suspension (harvested from cultures at the exponential phase). The six control wells contained 180 μL of the supplemented K medium and 20 μL of the heat-killed *E. coli* OP50 suspension. Approximately 1 μl of synchronized *C. elegans* at the L4 development stage were pipetted per well. The actual number of worms was determined visually with the aid of a stereomicroscope. Plates were incubated at 20°C and the morphological appearance were checked daily and *C. elegans* were counted with the aid of a Stemi 2000-C stereomicroscope (ZEISS).

4.5. Determination of lipid nanoparticle toxicity

The evaluation of the toxicity of lipid nanoparticles were tested *in C. elegans.* Aliquots of 50μL of nanoparticles were dispersed over the surface of individual plates containing *E. coli* OP50. L2 stage *C. elegans* were then transferred to these plates and incubated at 25ºC. Appearance of the worms was cheeked with the aid of a Stemi 2000-C stereomicroscope (ZEISS). Formulations tested were NLC_1, NLC_4 and NLC_5.

4.6. Determination of nanoparticle ingestion by *C. elegans*

A total of 1 mg of fluorescent dye DioC18(3), per 20mL of solution, was incorporated in formulation NLC_4, NLC_TOB and NLC_CIP. DioC18(3) is a green fluorescent, lipophilic carbocyanine and is widely used as a lipophilic tracer.

50 µl of each formulation were dispersed over the surface of individual agar plate containing *E. coli* OP50 and were air-dried for one hour. L4 stage *C. elegans* were then transferred to these plates. After 3h adult worms were transferred with 1 ml of M9 buffer to tubes and centrifuged (1 minute, 3000 rpm). Supernatant was discarded and 1ml of NaN_3 1mM was added. NaN_3 stop the digestive system of the worms and immobilize them. After 2 minutes, suspension was centrifuged once again (1 minute, 3000 rpm). 10 µl of the pellet was visualized in a fluorescence microscope Zeiss axioplan with 10x of magnification.

4.7. Nanoparticles with encapsulated ciprofloxacin efficacy assessment

50 µL aliquots of suspension of pathogens *B. contaminans* IST408, *B. cenocepacia* K56-2 and non-pathogenic *E. coli* OP50 were prepared from overnight growth cultures. These bacterial suspensions were plated onto the surface of 35 mm diameter petri plates containing 4ml of NGM II and then incubated for 24h. Aliquots of 50µL of nanoparticles with the antibiotic ciprofloxacin (diluted for the concentration of 32µg/mL) were dispersed over the surface of individual plates containing *B. contaminans* IST408, *B. cenocepacia* K56-2 and a negative control of non-pathogenic *E. coli* OP50. Approximately 20 hypochlorite-synchronized *C. elegans* BN2 larvae at the L2 development stage were pipetted per plate. The actual number of worms were determined visually with the aid of a stereomicroscope. Controls of empty nanoparticles and plates without nanoparticles were also tested. Each condition was performed in multiples of five and all the assay was performed in triplicate.

Plates were incubated during 3 days at 20°C. The morphological appearance, the ability to generate descendants and the percentage of live worms were checked daily.

The Nematode Growth Medium II (NGM II) contained per liter of distilated water, 3g NaCl, 2,5g peptone, 17g agar, 5 mL of nystatin (10mg/mL in ethanol), 25 mL of 1M K3PO4 buffer (pH6), 1 mL of 1M CaCl2, 1 mL of 1M MgSO4, 1 mL uracil (2mg/mL) and 0.5 mL cholesterol (10mg/mL in ethanol).

4.8. Antibiotic susceptibility testing

The Minimal Inhibitory Concentration (MIC) of the antibiotics used was determined using the broth dilution technique. For that, stock solutions of ciprofloxacin and tobramycin were prepared in Mueller Hinton (MH) liquid medium (Sigma-Aldrich) at a final concentration of 2048 mg/L. A 96-well plate was prepared containing in each well 100 µL of MH liquid medium. Sequential 1:2 dilution of each antibiotic was carried out in order to obtain final concentrations ranging from 1024 mg/L to 0.125 mg/L. The wells were then inoculated with 100 µL of the bacterial species to be tested with an initial optical density ($OD_{640\ nm}$) of 0.02 and incubated for 24 hours at 37ºC. After incubation, the bacterial growth was

determined based on the medium turbidity and the optical density of each well was measured in a SPECTROstar Nano microplate reader (BMG Labtech) at 640 nm. Positive (without antibiotic) and negative controls (no bacterial inoculum) were carried out.

5. Results and Discussion

5.1. Characterization of lipid nanoparticles

5.1.1. Size and zeta potential

The different formulations prepared for nanoparticles production are summarized in table 7. These nanoparticles were analysed with dynamic light scattering to determine the average size, PdI and zeta potential. The pH of the nanoparticles suspension prepared with different formulations was also measured.

Table 7: Composition of different formulations of prepared nanoparticles.

Formulation	Surfactant	Cosurfactant	Fatty acid	Oil
NLC_1	Tween 80	Hexadecane	Lauric acid + Myristic acid	Coconut oil
NLC_2	Span 80			
NLC_3	Tween 80		Stearic acid	
NLC_4		-		Sunflower oil
NLC_5	Span 80		Lauric acid	
NLC_6			Myristic acid	
NLC_7			Palmitic acid	

The results obtained for the determination of the average size and PdI are shown in figure 9.
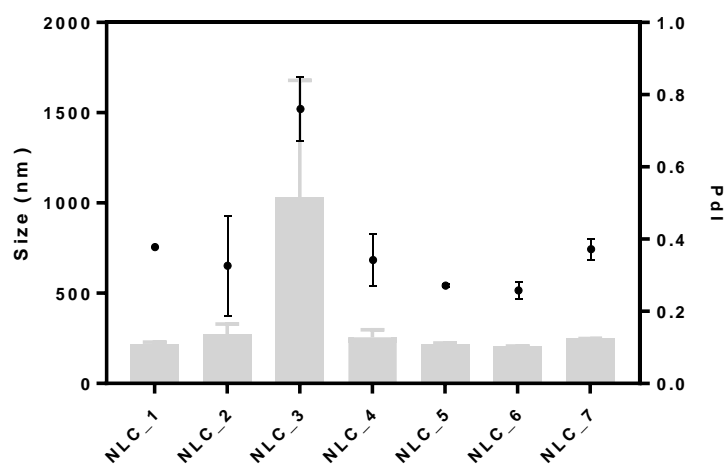
Figure 9: Characterization of the average size (vertical bars) and PdI (black dots) of the empty nanoparticles prepared with formulations NLC_1 to NLC_7.

The initial formulation used in this work (NLC_1)[69,70] was produced without recurring to sonication. These nanoparticles presented an average size of 219.0±11.0nm and PdI of 0.400±0.04. However, this formulation was excluded due to lower melting point of the nanoparticles (see chapter 5.1.2) and the extreme toxicity towards *C. elegans* (see chapter 5.3).

Experiments with nanoparticles containing a single fatty acid were performed without sonication and the resulting suspension formed visible aggregates; thus, the sonication step was added to the preparation of these nanoparticles (formulation NLC_2 to NLC_7).

Nanoparticles containing Tween 80 and stearic acid (formulation NLC_3) presented a large size (668.1±232.6nm) and a high value of polydispersity index (0.840±0.08). As already mentioned, PdI measure the size distribution of the nanoparticles. Higher PdI values indicate a higher polydispersity of the dispersion which is not desirable due to the different sizes of nanoparticles in the medium.

Results obtained for the determination of the zeta potential of the formulations NLC_1 to NLC_7 as well as the pH are shown in figure 10.
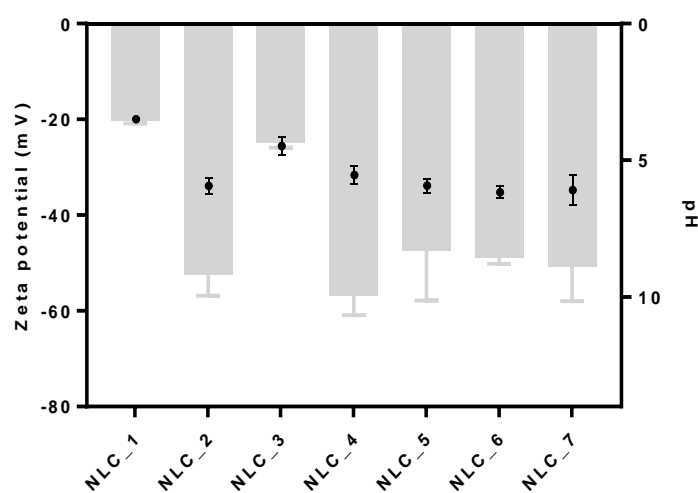
Figure 10: Zeta potential (vertical bars) and pH (black dots) of empty nanoparticles NLC_1 to NLC_7.

The zeta potential (ZP) indicates the overall charge that a particle acquires in a specific medium.

Nanoparticles containing Tween 80 (Formulations NLC_1 and NLC_3) presented a low zeta potential value, -20.3 ±0.52mV and -24.1± 0.65mV, respectively. These values predict a long term instable nanoparticles (Figure 10). Low ZP values (negative or positive) predict the attraction of the nanoparticles and they can flocculate or coagulate[26]. In opposition, values ranging from -47,5±0.90 mV to -56,9±3.72 mV were determined for nanoparticles formulated with surfactant Span 80, suggesting higher stability. High ZP values predict the prevention of aggregation of the nanoparticles due to electric repulsion. Generally, nanoparticles whose ZP values are not comprehended between -30mV and +30mV are considered stable[26]. Differences of the zeta potential between nanoparticles containing different surfactants could be due to the different pH of the final nanoparticles solution. Zeta potential is strong dependent of the pH of the solution. The pH of the suspension of nanoparticles with Tween 80 ranging from 3.5±0.08 to 4.48±0.32 and for suspension of nanoparticles with Span 80 ranging from 5.93±0.29 to 6.16±0.21. The medium with Span 80 is less acidic, therefore, the nanoparticles tend to acquire a more negative charge.

The choice of surfactant has an impact on the quality of the nanoparticles. Both surfactants used are non-ionic but present different HBL values. Tween 80 has a high HBL value (15.0) and Span 80 has a low HBL value (4.3)[74]. Consequently, Tween 80 has a high ratio of hydrophilic groups to lipophilic groups compared to Span 80. As aforementioned, surfactants with a low HLB number (3-6) are predominantly

hydrophobic, dissolve preferentially in oil, stabilize water-in-oil emulsions, and form reverse micelles in oi. A surfactant with a high HLB number (10-18) is predominantly hydrophilic, dissolves preferentially in water, stabilizes the oil-in-water emulsion, and forms micelles in water[25].

No significant differences were observed in average size, PdI or ZP in nanoparticles formulated with the different oils (sunflower oil-NLC_4 and coconut oil-NLC_2).

Formulations NLC_4, NLC_5, NLC_6 and NLC_7 were formulated with sunflower oil and span 80 but with different saturated fatty acids. No significant difference was observed in size, PdI and zeta potential of nanoparticles formulated with fatty acid with different length chain.

Taking into account the considerations above, the formulation NLC_4 was chosen, due to good size and polydispersity index and high zeta potential which predict a long-term stability.

The nanoparticles obtained exhibited a milky appearance, and an image of formulation NLC_4 is shown in figure 11.

Figure 11: Photograph of a vial containing nanoparticles suspension prepared with formulation NLC_4.

Antibiotics ciprofloxacin and tobramycin were encapsulated in nanoparticles obtained with formulation NLC_4. The average size, PdI and ZP obtained for these nanoparticles are presented in figure 12.

A 5 mg of antibiotic was added in each formulation (0.25 mg/mL). The size and the polydispersity index of the nanoparticles containing the antibiotics ciprofloxacin (258.5±50.7nm;0.399±0.08) and tobramycin (255,2±63.5nm;0.324±0.09) was similar compared to empty nanoparticles (255.9±40.8nm; 0.342±0.06).

The ZP of ciprofloxacin loaded nanoparticles (-48.9±4.09mV) is slightly lower that the empty ones (-56,9±3.72mV).

However, nanoparticles loaded with tobramycin exhibited a significant decrease of the zeta potential (-22.0±3.62mV). The pH of the tobramycin loaded nanoparticles increase (pH=7.58±0.13) in comparison with empty nanoparticles (5.53±0.34). Considering the basic character of tobramycin, and the increasing of pH in the suspension of nanoparticles loaded with tobramycin was expected the observation of the increasing of zeta potential due to the more negative charged medium. We hypothesize that tobramycin may be binding to the surface of the particle, conjugated with the stearic acid. Tobramycin is composed by 5 primary amino groups that could be binding to the carboxyl groups of fatty acids.
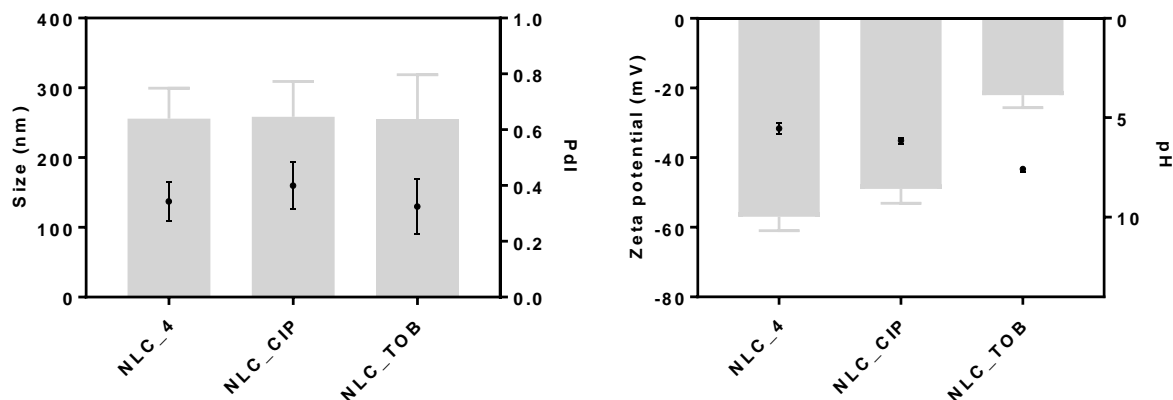
Figure 12: Average size (vertical bars), PdI (black dots), zeta potential (vertical bars) and pH (black dots) of nanoparticles loaded with ciprofloxacin (formulations NLC_CIP), tobramycin (formulation NLC_TOB) and empty nanoparticles (formulation NLC_4).

Different concentrations of each antibiotic (0.25 mg/mL, 0.5 mg/mL and 1 mg/mL) were also incorporated in the nanoparticles (Figure 13). No significant variations were observed in the average size, PdI and zeta potential of nanoparticles, except the increase of the size of nanoparticles with 1mg/mL of ciprofloxacin. Is also observed a tendency of increasing the size of nanoparticles with the increase concentration of both antibiotics.
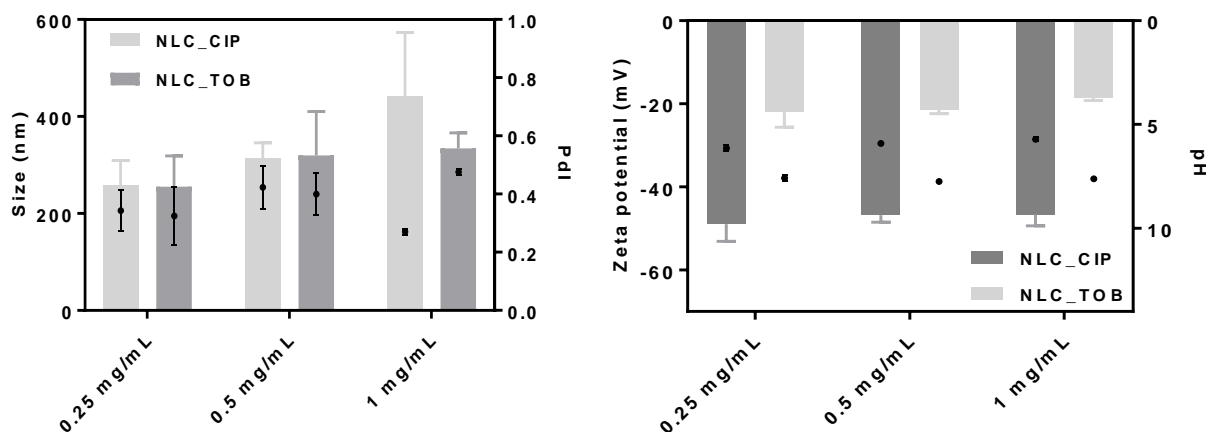
Figure 13: Average size (vertical bars), PdI (black dots), zeta potential (vertical bars) and pH (black dots) of nanoparticles loaded with ciprofloxacin (formulations NLC_CIP) or tobramycin (formulation NLC_TOB) loaded with 0.25, 0.5 or 1 mg of antibiotic.

Nanoparticles prepared from formulations NLC_4, NLC_CIP and NLC_TOB were stored at room temperature for two months and their size, PdI and zeta potential was assessed after one and two months of preparation (Figure 14). Results indicate that, in both formulations, nanoparticles were stable for at least 60 days. The nanoparticles average size slightly decreased in both nanoparticles formulations, due to the deposition of the nanoparticles. Zeta potential also decreased with time.
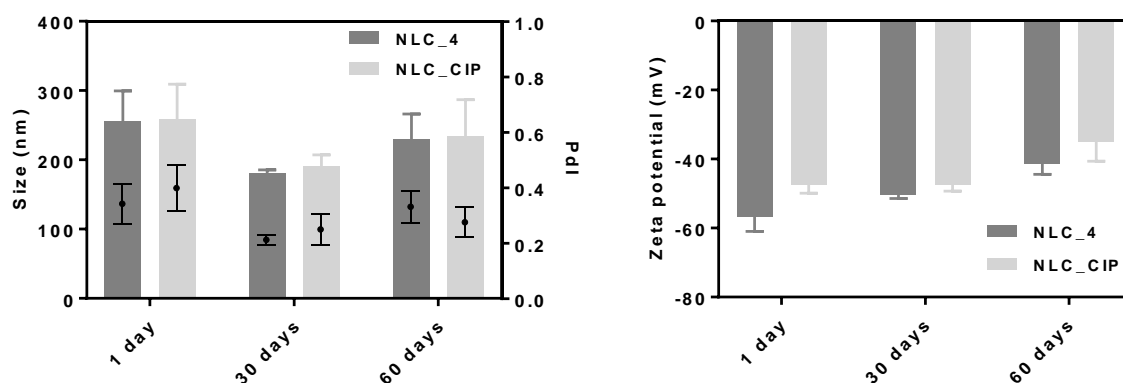
Figure 14: Size (vertical bars), PdI (black dots) and zeta potential (vertical bars) of nanoparticles obtained with formulation NLC_4 and NLC_CIP measured after 1, 30 and 60 days after production.

For the nanoparticles loaded with tobramycin, a phase separation in the suspension was detected after one month (Figure 15). Therefore, we conclude that these nanoparticles are not long-term stable, which is in agreement with the zeta potential measurements previously obtained (Figure 12).

Figure 15: Photograph showing the visual aspect of vials containing empty nanoparticles (left) or loaded nanoparticles with tobramycin after 1 month (right).

A fluorescent dye was also encapsulated in formulation NLC_4 together with ciprofloxacin or tobramycin in order to investigate if the worms ingested or not the nanoparticles (see chapter 5.4). The average size, PdI and zeta potential of these nanoparticles is shown in table 8. These nanoparticles were larger in size (20% to 30% higher) and exhibited a higher polydispersity index when compared to empty nanoparticles.

Table 8: Average size, PdI and zeta potential of nanoparticles prepared with formulations NLC_4, NLC_CIP or NLC_TOB together with dye Dio.

	Size (nm)	PdI	Zeta potential (mV)
NLC_Dio	334.9±5.251	0.608±0.047	-50.3±1.80
NLC_DioCIP	309.0±11.15	0.552±0.092	-52.8±0.777
NLC_DioTOB	321.7±6.907	0.405±0.028	-22.9±0.451

5.1.2. Differential scanning calorimetry

Nanoparticles prepared without recurring to sonication (formulation NLC_1) were composed of a mixture of fatty acids (lauric acid and myristic acid). No melting event was observed with nanoparticles of this formulation. When the individual components were tested, the melting temperature of this mixture of fatty acids significantly decrease (figure 16). Myristic acid and lauric acid have melting temperatures of 56.3ºC and 46.5ºC, respectively. When mixed, the melting temperature drops to 37.2ºC. Based on differential scanning calorimetry, Keles S. et al. (2005), reported that the lauric acid and myristic acid are phase change materials that have a high melting point. However, their melting point can change when mixed, forming a eutectic mixture[75]. This phenomenon was also observed for other mixtures of fatty acids such as lauric acid and palmitic acid[76], stearic acid and lauric acid[77]. Thus, this formulation it's closer to nanoemulsion than nanostructured lipid carrier because is not solid at body temperature.
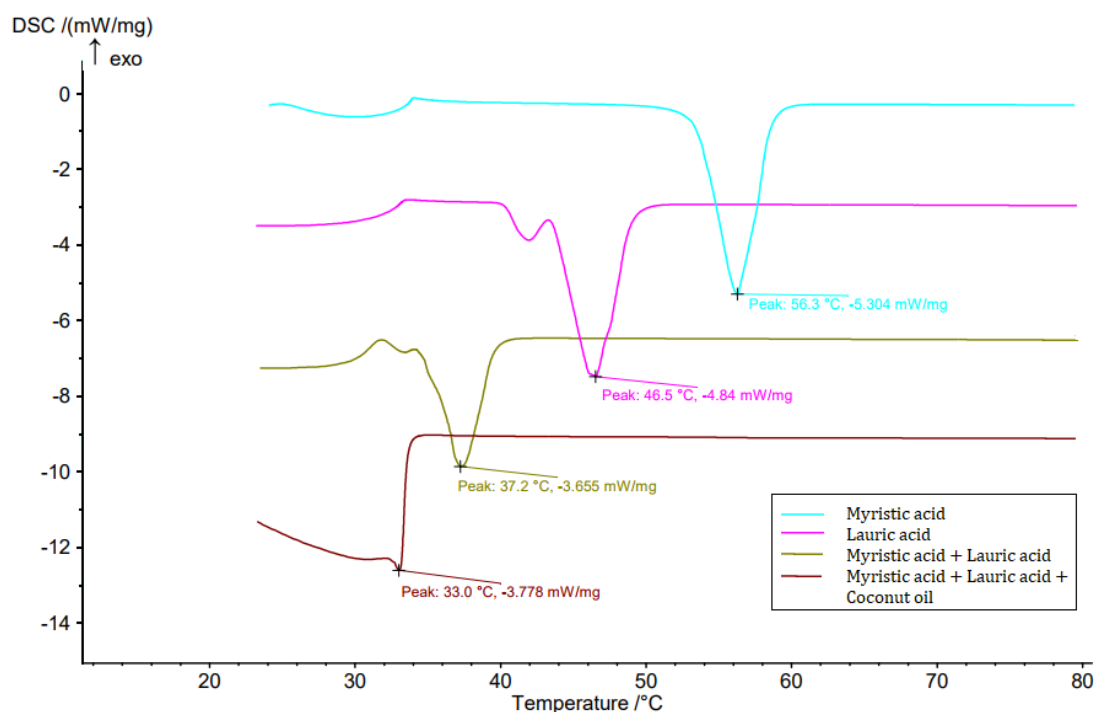
Figure 16: DSC analysis of the individual solid compounds (lauric acid or myristic acid) and a mixture of a lipids (lauric acid and myristic acid) and (lauric acid, myristic acid and coconut oil).

Empty nanoparticles prepared recurring to a sonication step (formulations NLC_2 to NLC_7) were analysed by differential scanning calorimetry. The melting points obtained for the nanoparticles prepared with the formulations NLC_2 to NLC_7 are summarized in table 9. No significant differences were observed for nanoparticles prepared with different surfactants (NLC_3 with Tween 80 and NLC_4 with Span 80) and with different oils (NLC_2 with coconut oil and NLC_4 with sunflower oil). Nanoparticles containing different fatty acids exhibited a trend towards the increase of melting temperatures with the length of the fatty acid chain, what is the expected due to the increase of melting temperature of the individual fatty acid. Nanoparticles of formulations NLC_5 and NL_6 are not solid at body temperature.

The increase of the amount of the solid lipid in the formulation and the decrease of oil content could be solution to this problem.

Table 9: Melting point of nanoparticles in the formulations NLC_2 to NLC_7.

Formulation	Temperature (ºC)	SD
NLC_2	58.1	0.95
NLC_3	59.9	0.50
NLC_4	58.9	2.25
NLC_5	32.2	1.30
NLC_6	36.5	1.00
NLC_7	55.3	0.60

Differential scanning calorimetry analysis was also performed only for the fatty acidic used in the formulations. Results are represented in annex 5.

Nanoparticles with antibiotics (formulations NLC_CIP and NLC_TOB) were also analysed by differential scanning calorimetry and the results obtained are shown in figure 17. Table 10 summarizes the melting temperatures for these nanoparticles. Nanoparticles containing both antibiotics present a melting point similar to that of empty nanoparticles (formulation NLC_4).
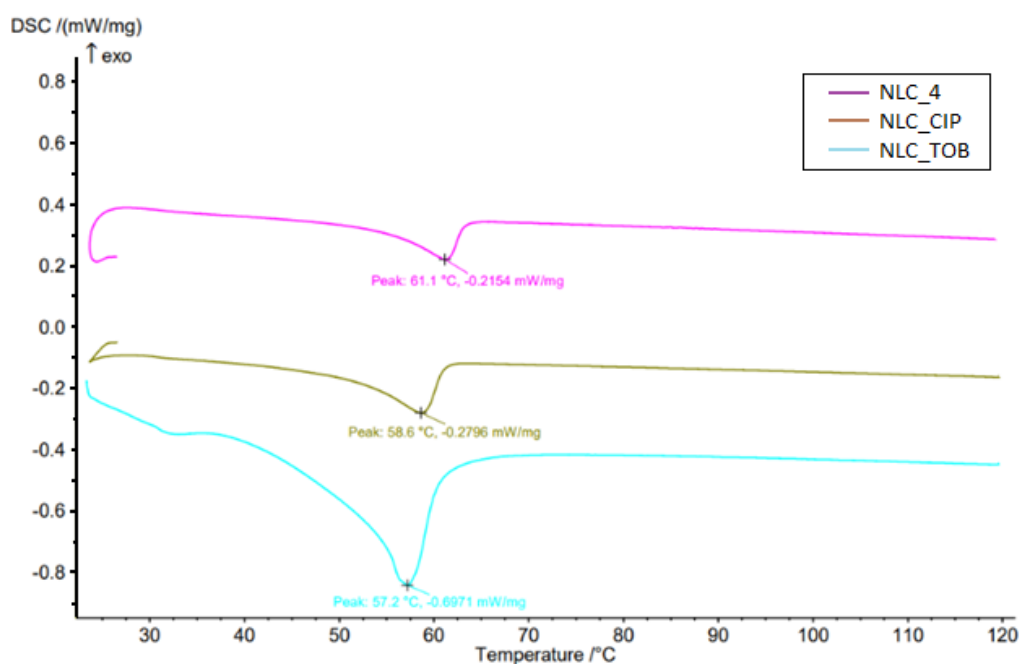
Figure 17: Melting point of nanoparticles loaded with the antibiotics ciprofloxacin (NLC_CIP) or tobramycin (NLC_TOB). Results for the empty nanoparticles (NLC_4) are also presented.

Table 10: Melting point of nanoparticles formulated with antibiotics.

Formulation	Temperature (ºC)	SD
NLC_CIP	59.5	0.85
NLC_TOB	56.9	0.30

5.1.3. Transmission electron microscopy observation

Transmission electron microscopy was used to observe the shape and morphology of lipid nanoparticles. TEM images of nanoparticles prepared with formulation NLC_1 is shown in figure 18.

Dynamic light scattering analysis shown that nanoparticles prepared with formulation NLC_1 had a mean particle size of 219±11.0nm and a PdI of 0.4±0.04. In the presented TEM images, some aggregations with an average size of 20 nm (Figure 18-A) and some spherical nanoparticles with sizes near 200 nm (Figure 18-B) were observed. This is not in agreement with the average values obtained in DLS measurements. Those aggregates were either considered as a single particle (with approximately 200 nm) or corresponded to some contamination. Overall the nanoparticles presented a spherical shape.
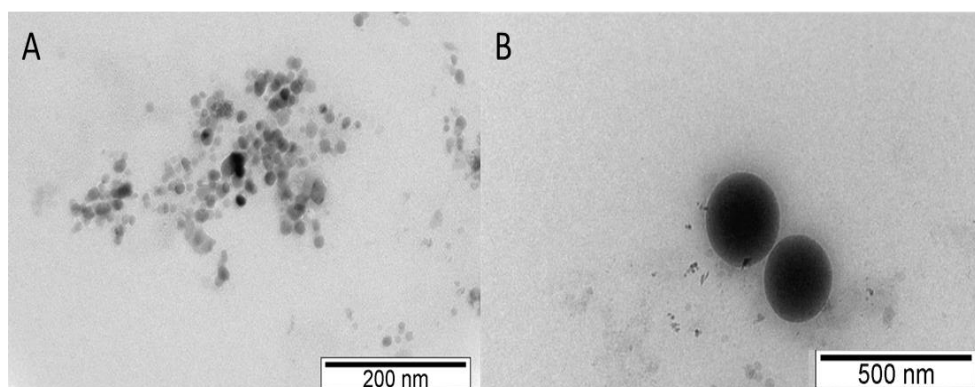
Figure 18: Transmission electron microscopy imagens prepared with formulation NLC_1.

The first TEM visualization of nanoparticles prepared with formulations NLC_4, NLC_CIP or NLC_TOB was not clear. The presence of some sort of film was observed masking the image and obstructing nanoparticles visualization (annex 6). This was presumably caused by the high lipophilicity of Span 80. To avoid this problem the nanoparticles were filtered and clearer images were obtained. figure 19 presents the TEM images obtained for empty nanoparticles (A), tobramycin loaded nanoparticles (B) and ciprofloxacin loaded nanoparticles (C).

Empty nanoparticles (A) and nanoparticles with tobramycin (B) presented a spherical shape and an average size of 200 nm, this is consistent with the dynamic light scattering data (255.9±40.8nm and 255.3±63.5nm, respectively).

Nanoparticles loaded with ciprofloxacin (C) were also filtered. Despite, the obtained images being less clear that the previous ones, it is still possible to observe the nanoparticles (presumably the dark spots) with sizes ranging from 100 nm to 200 nm. Again, this values are consistent with the DLS data (258±50.7nm).
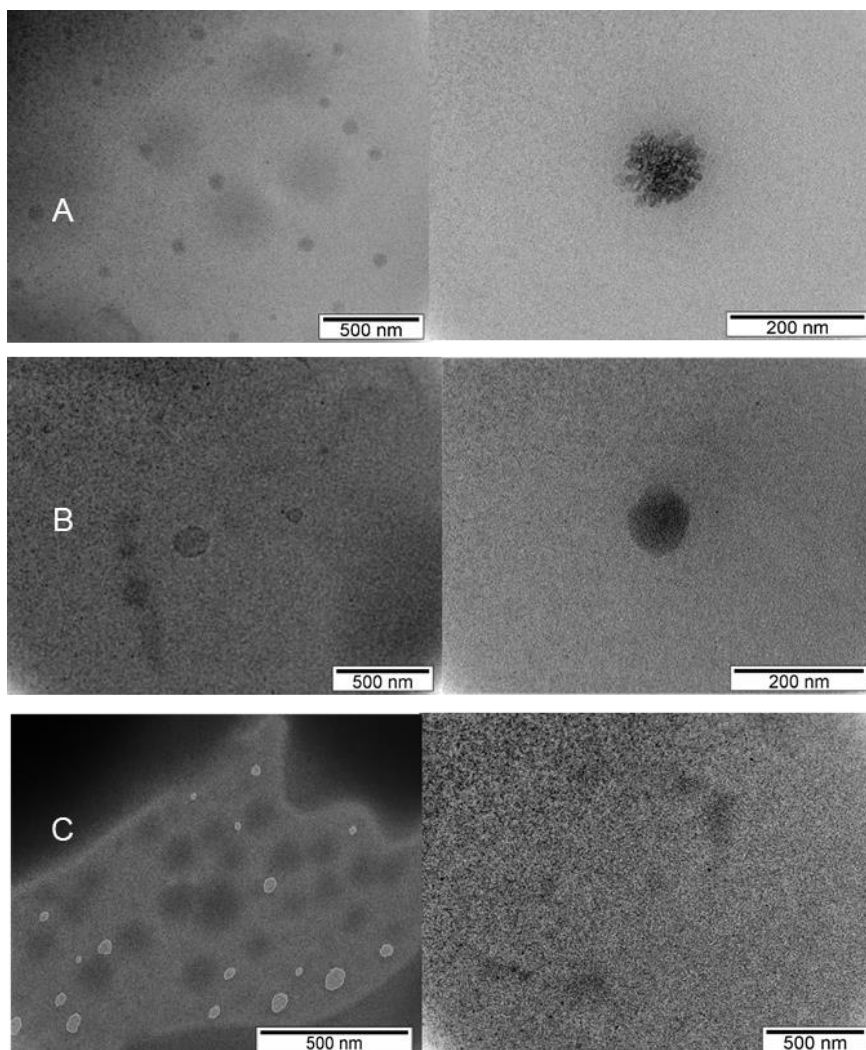
Figure 19: Transmission electron microscopy images of empty nanoparticles (A) (formulation NLC_4), nanoparticles loaded with tobramycin (B) (formulation NLC_TOB) and nanoparticles loaded with ciprofloxacin (C) (formulation NLC_CIP).

5.1.4. Encapsulation efficiency and drug loading

Encapsulation efficiency was calculated by the quantification of ciprofloxacin presented in the filtrate that was obtained through filtration of the nanoparticle suspension. To confirm if antibiotics were or not retained in the membrane, a known concentration of each antibiotic was analysed before and after the filtration procedure (table 11).

Table 11: Quantification of free antibiotics ciprofloxacin before and after the filtration step in Spin-X® UF centrifugal filter device.

	Area before filtration	Area after filtration
Ciprofloxacin	26348535	26285730
	Intensity of fluorescence before filtration	**Intensity of fluorescence after filtration**
Tobramycin	54.76	48.6

To verify if nanoparticles maintained the same average size, PdI and zeta potential, the formulations were analysed before and after the filtration. Results presented in table 12 indicate that after filtration nanoparticles decreased in average size, PdI and zeta potential. This suggest that the larger nanoparticles can be retained in the membrane.

Table 12: Average size, PdI and zeta potential of nanoparticles loaded with ciprofloxacin (formulations NLC_CIP) or tobramycin (formulation NLC_TOB) before and after filtration.

	Size (nm)	PdI	Zeta Potential
NLC_CIP before filtration	253.45±13.93	0.384±0.006	-52.8±2.687
NLC_CIP after filtration	202.10±28.28	0.260±0.073	-46.10±2.969
NLC_TOB before filtration	316.30±78.63	0.405±0.031	-26.70±0.565
NLC_TOB after filtration	264.35±56.92	0.334±0.021	-21.95±0.353

Filtrates resulting from the filtration of tobramycin loaded nanoparticles had no absorbance (with a blank of water + fluorescamine) neither intensity of fluorescence (with a blank of phosphate buffer + fluorescamine), suggesting that there was no antibiotic in the filtrate. To verify if the tobramycin was retained in the membrane of filter devices, the free antibiotic was quantified before and after the filtration (Table 10). The fluorescence Intensity decrease after the filtration procedure but with no significant difference. To verify if the high temperature or sonication procedure damaged the antibiotic, the intensity was measure before and after the heating step. After the heating and sonication step, the fluorescence intensity of the antibiotic remained similar.

Results seems to show an unexpectedly high encapsulation efficiency of 100%. This may be possible due to the 5 primary amino groups that tobramycin presents, these can associate to carboxylic group of the stearic acid, improving the encapsulation yield. However more studies should be performed to determine what occur with this antibiotic and its quantification.

5.1.4.1. Ciprofloxacin

Different concentrations of the antibiotic ciprofloxacin were incorporated in nanoparticles. Figure 20 shows the different encapsulation efficiencies and drug loading with different concentrations of ciprofloxacin (0.25, 0.5 and 1mg/mL).
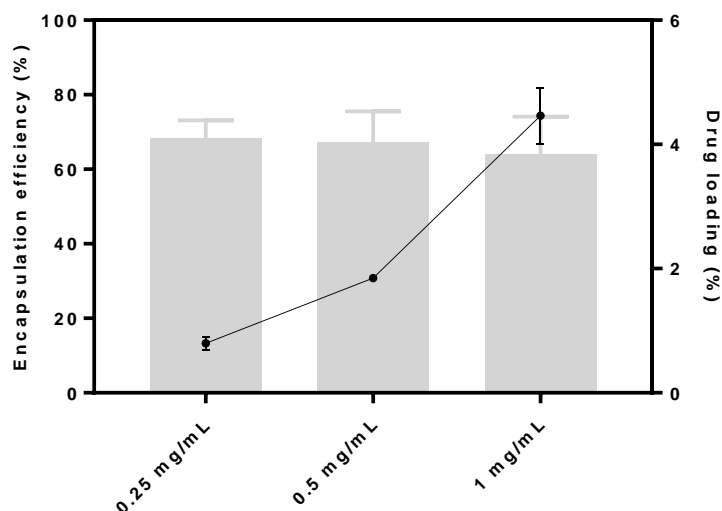
Figure 20: Encapsulation efficiency (vertical bars) and drug loading (black dots) of nanoparticles loaded with different ciprofloxacin concentrations (0.25, 0.5 and 1mg/mL).

Encapsulation efficiency was calculated by the quantification with HPLC of filtrates resulting from the filtration of loaded nanoparticles. Encapsulation efficiencies of nanoparticles loaded with 0.25, 0.5 and 1mg/mL of ciprofloxacin (formulation NLC_CIP) was 68.16±4.9%, 67.26±8.27% and 64.11±9.99%, respectively while drug loading capacity was 0.79±0.10%, 1.84±0.03% and 4.46±0.44%, respectively. The amount of antibiotic added to the formulation was 5mg for 400 mg carrier to 20mg for 400mg carrier.

Furthermore, additional studies should be performed to determine the maximum drug loading capacity of the lipid nanoparticles of these formulations, this is, the maximum amount of antibiotic that can be incorporated in nanoparticles.

Dharmendra Jain et al.[32], obtained an EE of 38.71%±2.38% to 8.66%±1.64% for SLN formulations with microemulsion technique (25mg/100mg carrier to 100mg/100mg carrier). Ghaffari et al.[33], obtained an EE% of 88±4.5% with emulsification-sonication method. Gamal A. Shazly[35] obtained for SLNs with stearic acid an EE of 73.94% with emulsification-sonication method.

The type of lipid used for the preparation of lipid nanoparticles has a significative impact on the encapsulation efficiency and drug loading capacity of the formulations. Other type of lipids could be used to optimize the maximum percentage of encapsulated drug.

5.1.5.   Drug release profile
5.1.5.1. Ciprofloxacin

Release studies were performed with dialysis tubing, that is a semi-permeable membrane which facilitated the exchange of molecules in solution. Nanoparticle suspension was added to the dialysis tubing and the exterior medium was composed of phosphate buffer (pH=7.4). Samples of the release medium were taken at different time points and ciprofloxacin in the medium was quantified by HPLC. Release of free antibiotic was also measured as control.

The release profile of ciprofloxacin from nanoparticles and free ciprofloxacin over time is represented in figure 21. The profile shows a burst release were all the drug is released in the first 7 hours (96% release at t=7h). The encapsulated antibiotic presented a similar release profile compared to free

antibiotic (95% release at t=3h). This result could suggest that the antibiotic is at surface of the particle. Table 13 shows the size and PdI of the formulation used in this study before and after the release which suggests that most of the nanoparticles have disrupted due the high average size and polydispersity index of the final suspension.

The drug could be associated to the nanoparticles in three different states: at the nanoparticle surface, in the core as a reversible complex, or in the core as irreversible complex. Generally, drug release follows more than one type of mechanism. In case of release from the surface, drug adsorbed on the surface of nanoparticles dissolves instantaneously when in contact with the release medium. The early phase of the release corresponds to the release of drugs physically bound to the surface of the nanoparticles. The delayed phase corresponds to the release of entrapped drug due to diffusion of drug from the rigid matrix structure[32].

The nanoparticle suspension used in this assay had an encapsulation efficiency of 69.62% and free antibiotic was not separated from the nanoparticles. Other approach could involve the washing of nanoparticles for more accurate results.
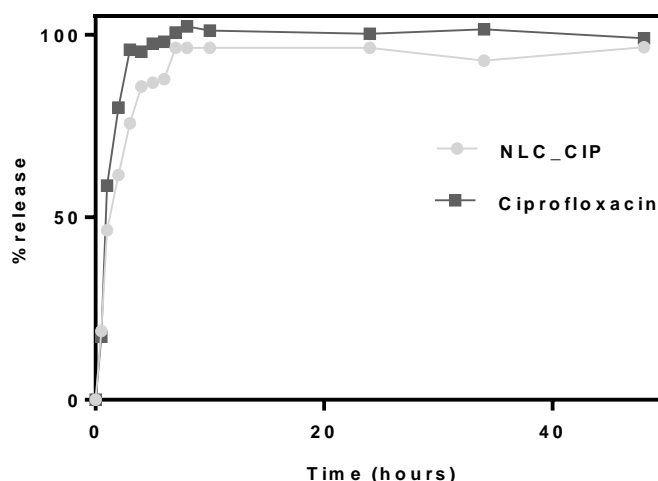
Figure 21: Release profile of ciprofloxacin from nanoparticles (Formulation NLC_CIP) and free ciprofloxacin over 48h.

Table 13: Characterization of one lipid nanoparticle formulation before and after the release profile study.

	Size (nm)	PdI
Initial NLC	230.4±1.652	0.363±0.028
Final NLC	777.15±732.3	0.678±0.288

Dharmendra Jain et al.[32], produced five different types of nanoparticles of albumin, gelatine, chitosan, and solid lipid nanoparticles with ciprofloxacin. In their results chitosan and gelatin nanoparticles can release the drug for as long as 96 h, whereas drug release through SLN was observed for up to 80 h. On the other hand, free ciprofloxacin hydrochloride showed a burst release with almost 50% free drug release in 30 min and more than 90% drug diffusing in 70 min[32]. Their results suggest that SLNs can act as promising carriers for sustained ciprofloxacin release. Gamal A. Shazly[35] produced SLNs with different lipids and nanoparticles formulated with only stearic acid as lipid component displayed the strongest burst effect and the most rapid released. Shazly proposed that this could be due to the fast

dissolution of ciprofloxacin molecules existing in the surface layer of the SLNs. Ghaffari et al.[33], also obtained a similar release of ciprofloxacin encapsulated in SNLs with a significant burst effect.

5.2. Toxicity assay in liquid medium of tobramycin and ciprofloxacin

Figure 22 shows the percentage of *C. elegans* survival in liquid medium containing different concentrations of ciprofloxacin (A) and tobramycin (B). Our results indicate that tobramycin has a higher toxic effect to the nematode when compared to ciprofloxacin. Tobramycin led to a decrease of nematodes survival from concentration of 2µg/ml (80%) to 256 µg/ml with a percentage of survival of 11.1% (Figure 22 B). Jeffrey et al. (2012), presented a study where *C. elegans* infected with pathogens (for example with *S. aureus*), were exposed to tobramycin with a concentrations equally low (1.25 µg/ml)[78]. Nematodes exposed to ciprofloxacin presented a maximum survival percentage for concentrations of the antibiotic up to 32 µg/ml, and even with the highest concentration tested (1024 µg/ml) a survival percentage close to 80% was registered (Figure 22 A).
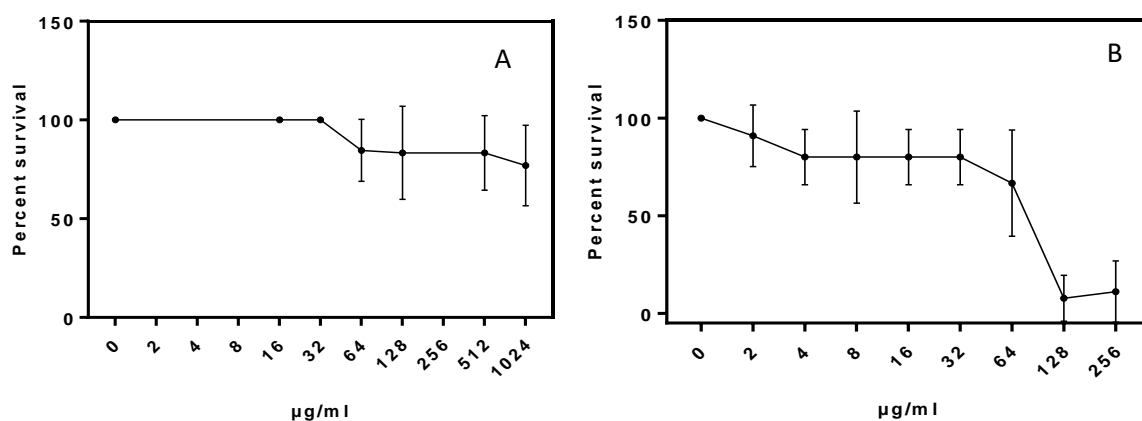
Figure 22: Percentage of *C. elegans* survival when cultivated upon exposure to different concentrations of ciprofloxacin (A) and tobramycin (B).

The visual inspection of the nematodes morphology with the aid of a stereoscope revelled that *C. elegans* were smaller when present in antibiotic enriched medium when compared to the six controls without antibiotic (data not shown).

5.3. Toxicity of lipid nanoparticles in *C. elegans*

In this work, the first nanoparticles tested in *C. elegans* were prepared by formulation NLC_1. This formulation showed to be extremely toxic to the nematodes. Worms died almost instantaneously when in contact with the nanoparticles and the same behaviour was observed with nanoparticles prepared with formulation NLC_5. These formulations had in common the lauric acid. Based on these results, we have presumed that this fatty acid was the cause of the nematodes mortality. Figure 23 shows an image of the worms after contact with nanoparticle prepared with formulation NLC_1. All observed worms were dead and had formed agglomerates.

Figure 23: Image of *C. elegans* after exposure of nanoparticles prepared with formulation NLC_1. No worms were alive after t=2min of nanoparticle exposure.

In 1994, Marc Stadler et al., investigated the fatty acids and other compounds that presented nematicidal activity to *C. elegans* at the L4 stage after 18h of exposure. They present values for LD_{50} (dose required to kill half of the members of a tested population) for *C. elegans.* Values for LD_{50} of fatty acids in their study were: lauric acid $LD_{50}=25$ μg/mL; myristic acid $LD_{50}=5$μg/mL; palmitic acid $LD_{50}=25$μg/mL and stearic acid $LD_{50}=50$μg/mL[79].

5.4. Assessment of nanoparticle ingestion by *C. elegans*

To determine if worms did ingest or not the nanoparticles, a fluorescent dye was incorporated in them. The dye was encapsulated together with each antibiotic, ciprofloxacin or tobramycin. Figure 26 shows the microscopic images of *C. elegans* after 3h of nanoparticle exposure. Green Light corresponds to nanoparticles loaded with the fluorescent Dye. Is possible to see that worms ingested the nanoparticles and the fluorescence is observed along the digestive system of the worms.

Remarkably, we have observed that only a few worms were fluorescent when tobramycin-containing nanoparticles were used, in opposition to the observed for ciprofloxacin.
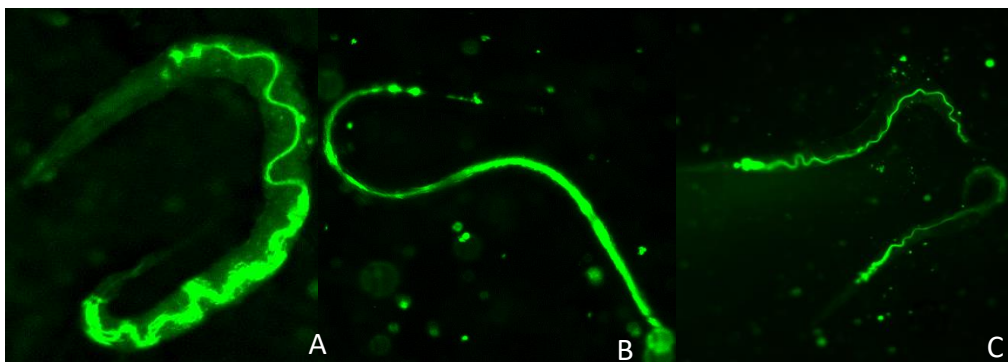
Figure 24: Microscopy images of *C. elegans* fed with nanoparticles containing fluorescent dye and the antibiotics ciprofloxacin or tobramycin. A- nanoparticles loaded with Dio; B- nanoparticles loaded with ciprofloxacin and Dio; C- nanoparticles loaded with tobramycin and Dio.

5.5. Nanoparticle efficacy assessment

5.5.1. Ciprofloxacin

We have compared the survival percentage of worms in non-pathogenic *E. coli* OP50 in the presence of nanoparticles with ciprofloxacin or empty nanoparticles. Control experiments with no nanoparticles were also carried out. Results are shown in figure 25.
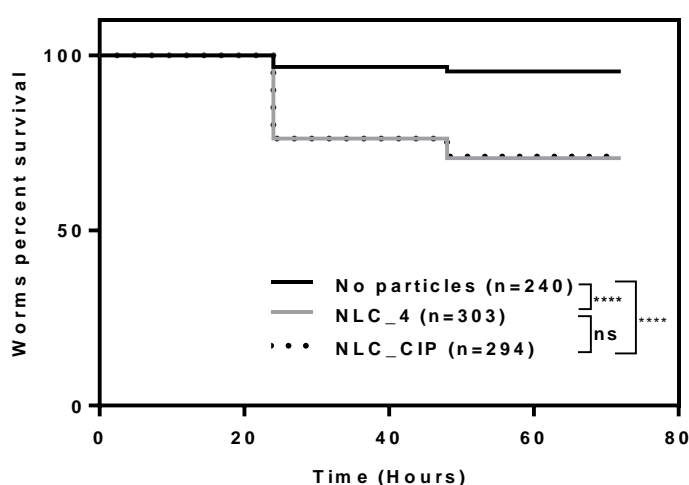
Concerning the survival of worms in *E. coli* OP50 (Figure 25), some mortality occurred among the worms exposed to empty nanoparticles (29.7%) and nanoparticles with ciprofloxacin (28.92%). The mortality of worms exposed to empty nanoparticles or to nanoparticles containing ciprofloxacin is not significantly distinct (P=0.9074). However, results obtained with each formulation tested is significant different for those obtained with no nanoparticles (P<0.0001). Altogether these results indicate that lipid nanoparticles present some toxicity to the worms.

Figure 25: Percentage survival of worms in the absenceof nanoparticles (-) or empty nanoparticles (formulation NLC_4) and nanoparticles with ciprofloxacin (formulation NLC_CIP) when fed with the non-pathogenic *E.coli* OP50. The survival curves were compared using the log-rank (Mantel-Cox) test and p-value is represented by: * when $P<0.05$; **when $P<0.01$; *** when $P<0.001$; **** when $P<0.0001$ or ns (not significant).

We have also assessed the survival percentage of infected worms with *B. contaminans* IST408 or *B. cenocepacia* K56-2 using the same conditions as those described above for *E. coli* OP50. The results obtained are shown in figure 26 and figure 27.

Infected worms with *B. cenocepacia* strain K56-2 (Figure 26) presented a mortality of 45.24% for the control with no nanoparticles, 38.71% in presence of empty nanoparticles and 36.87% in presence of nanoparticles with ciprofloxacin. According to the statistic model using the log-rank (Mantel-Cox) this small difference observed is not significant. In a study published by Cardona et al., in 2005, the percentage of survival of worms infected with *B. cenocepacia* K56-2 was 22% at day 2[80]. The difference of percentage compared with this assay is possibly due to different stages of the *C. elegans* used (L2 larval stage worms were used in this study while Cardona used L4 stage worms).

After 3 days, a visual inspection of the worms revelled that the infected worms with *B. cenocepacia* K56-2 were visibly smaller compared to those fed with *E. coli* OP50.Worms in both conditions laid eggs after this period.
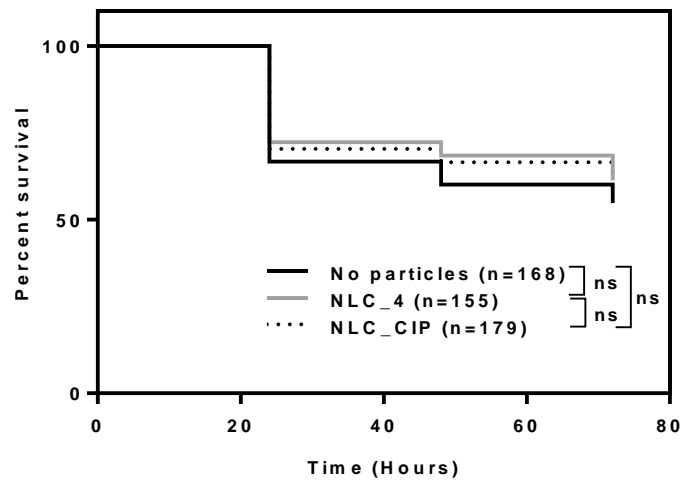
Figure 26: Percentage survival of worms infected with *B. cenocepacia* K56-2 in the absence of nanoparticles (**-**), empty nanoparticles (NLC_4) or nanoparticles with ciprofloxacin (NLC_CIP). The survival curves were compared using the log-rank (Mantel-Cox) test and p-value is represented by: * when P<0.05; ** when P<0.01; *** when P<0.001; **** when P<0.0001 or ns (not significant).

Similar experiments were carried out using worms infected with *B. contaminans* IST408 (Figure 27). Results obtained show that infected worms presented a mortality of 84.5% for control without nanoparticles, 87.8% for control with empty nanoparticles, and 77.5% for nanoparticles with the antibiotic ciprofloxacin, after 3 days. The difference observed in worm mortality in absence of nanoparticles or nanoparticles with ciprofloxacin is significantly different according to the statistic model using the log-rank (Mantel-Cox) (p-value=0.0410). The difference is more evident comparing the survival of worms in presence of empty nanoparticles or nanoparticles with the antibiotic (p-value=0.0018).
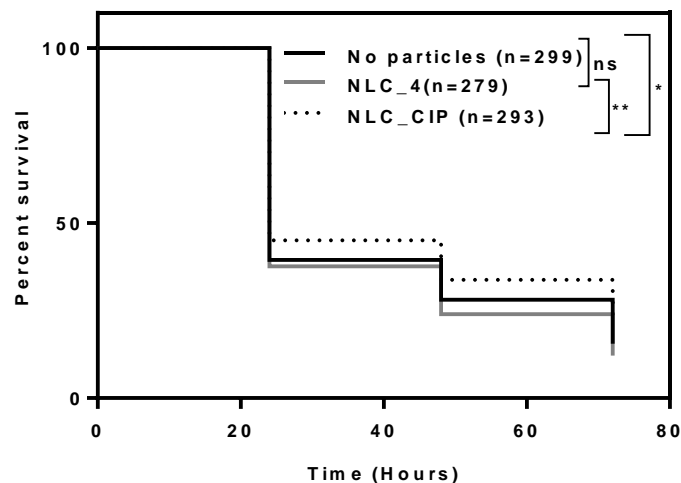
Figure 27: Percentage survival of *B. contaminans* IST408-infected worms in the absence of nanoparticles (**-**) or in presence of empty nanoparticles (formulation NLC_4) and nanoparticles with ciprofloxacin (NLC_CIP). The survival curves were compared using the log-rank (Mantel-Cox) test and p-value is represented by * when P<0.05, **when P<0.01*** when P<0.001, **** when P<0.0001 or ns (not significant).

The percentage of mortality of *C. elegans* by *B. contaminans* strain IST408 was previous reported by Sousa et al., (2010) (80%); The differences in the survival rates might be due to the fact that the strain of *C. elegans* used by those authors,DH2, was different from the ones in this study, BN2[81].

Worms were visible infected in the 3 conditions, being considerable smaller than those fed with *E. coli* OP50.

C. elegans presents many advantages, among them the fact that oral absorption is the main route of drug administration in worms. Thus, in this study, worms were used as *in vivo* animal model for evaluate the oral absorption as well as toxicity and efficacy of lipid nanoparticles. Despite nanoparticles presented some toxicity for *C. elegans*, the used components such as fatty acids (lauric acid, myristic acid, palmitic acid and stearic acid) are direct food substances affirmed as generally recognized as safe, according to FDA. Likewise, Span 80 and Tween 80 are used as food additives permitted for direct human consumption[82].

5.6. Antibiotic susceptibility testing

To validate the observed difference in the survival rate of the infected nematodes with the different pathogens in the presence of nanoparticles with ciprofloxacin, the minimal Inhibitory concentration (MIC) of the antibiotics (ciprofloxacin and tobramycin) was determined for the two strains under study, at the exponential phase of growth (Figure 28).
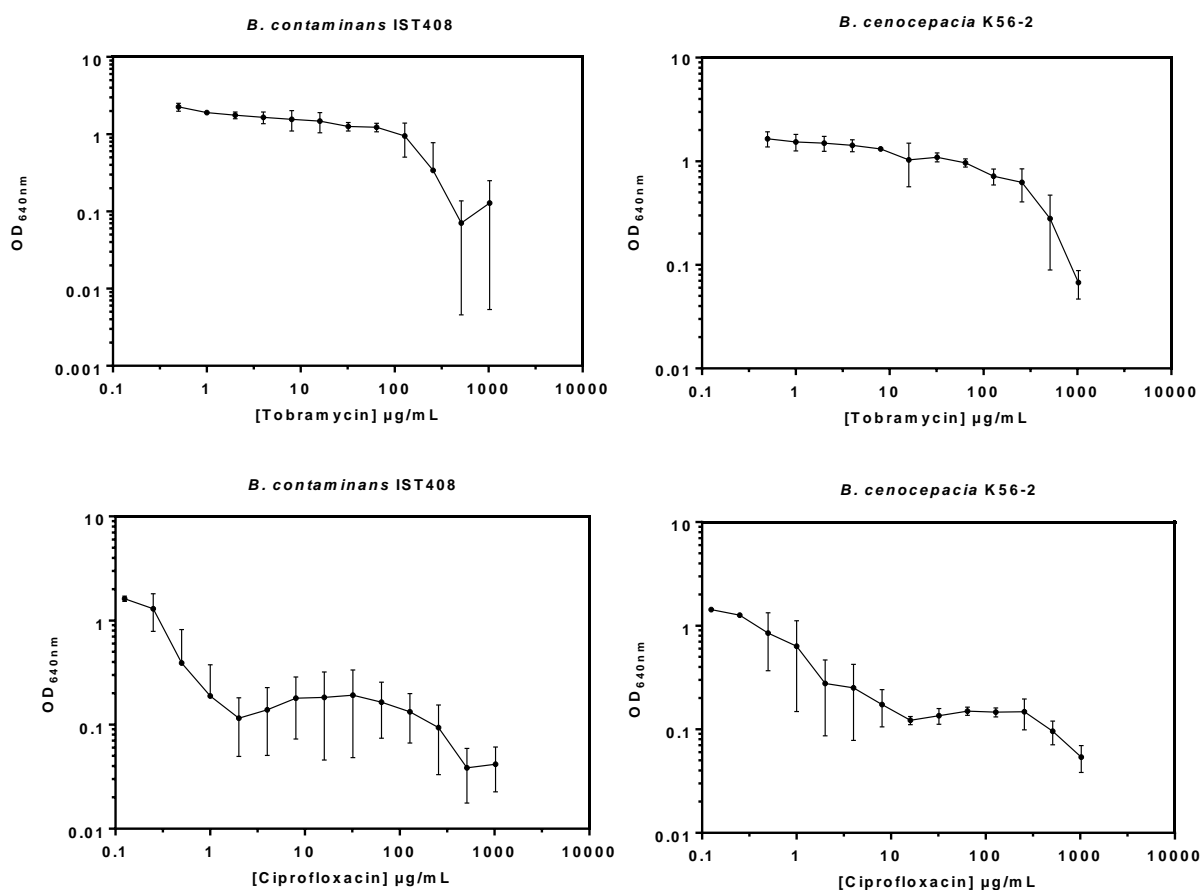
Figure 28: Antibiotic susceptibility test in *B. contaminans* IST408 and *B. cenocepacia* K56-2.

The MIC values estimated for ciprofloxacin towards *B. contaminans* IST 408 was 0.579 µg/mL, while for *B. cenocepacia* K56-2 was 2.66 µg/mL. Tobramycin MIC value for *B. contaminans* IST 408 was 5300

µg/mL, while for stain *B. cenocepacia* K56-2 this antibiotic showed no efficacy for the concentrations tested.

The amount of antibiotic ciprofloxacin in nanoparticles used in rescue experiments with infected *C. elegans* was 32 µg/mL. Our results indicate that ciprofloxacin is more effective against *B. contaminans* IST408 that against *B. cenocepacia* K56-2, in good agreement with results of rescue experiments with infected *C. elegans*. However, for the concentration 32 µg/mL it was expected to observe some differences in *B. cenocepacia* K56-2 survival. Nevertheless, the effective antibiotic concentration in the worm's intestine could be much lower than that that was applied at surface of the plates, since it depends on the ingestion of the nanoparticles by the nematode.

For future studies, different pathogens have to be chosen for the assessment of the efficacy of nanoparticle with tobramycin since tobramycin is not very effective in these strains (*B. cenocepacia* K56-2 and *B. contaminans* IST408).

6. Conclusions and Future work

The first part of this work consisted on the design and optimization of a nanostructured lipid carrier formulation. A final formulation (NLC_4) was successfully prepared by an emulsification-sonication technique. These formulations were composed of stearic acid, sunflower oil, Span 80 and milli-Q water and the nanoparticles obtained exhibited an average size of 255.9±40.8nm, PdI of 0.342±0.06 and zeta potential of -56.0±3.72 mV. The sonication procedure results in some disadvantages such as difficulty in scale up and metal contamination coming from the tip.

Nanoparticles with ciprofloxacin and tobramycin presented an average size and PdI similar to those of empty nanoparticles. However, the zeta potential of nanoparticles with tobramycin was much lower suggesting, that these nanoparticles are less long-term stable. Stability studies proved that the nanoparticles with ciprofloxacin were stable up to two months opposition to the observed for tobramycin loaded nanoparticles where the emulsion had break and two phases were visible after one month. Lyophilization and spray drying are good examples of alternatives for lipid nanoparticles storage for long periods of time, preventing degradation reactions such as hydrolysis and allowing the maintenance of the initial nanoparticle size. Transmission electron microscopy provided images of nanoparticles with spherical shape and with a size of approximately 200 nm.

A burst release of ciprofloxacin from the nanoparticles was verified (all the drug was released in the first 7hours), similar to free antibiotic. This suggests that antibiotic is at the surface of the lipid nanoparticle. Encapsulation efficiency of these nanoparticles was between 68.16±4.9% and 64.11±9.99% and drug loading 0.79±0.10% to 4.46±0.44%. The type of lipids, oils and surfactants used for the preparation of lipid nanoparticles has a significative impact on the encapsulation efficiency and drug loading capacity of the formulations. Other type of formulations could be used to optimize the maximum percentage of encapsulated drug.

Thermal analysis showed a melting temperature of 58.9ºC±2.25ºC, 59.5±0.05ºC and 56.9±0.30ºC for the nanoparticles of formulations NLC_4, NLC_CIP and NLC_TOB, respectively. These nanoparticles are solid at room temperature as well as at body temperature.

Caenorhabditis elegans was used as an animal model of infection and pathogens belonging to the Bcc group were used as model pathogens (*Burkholderia contaminans* IST408 and *Burkholderia cepacia* K56-2). In the first strain, significant differences were observed between nanoparticles with ciprofloxacin or the control without nanoparticles (p-value<0.05) and between empty nanoparticles or nanoparticles with the antibiotic (p-value<0.01). In the case of *B. cenocepacia* K56-2 no significant difference was observed in the rescue experiments without nanoparticles and antibiotic loaded nanoparticles.

Fluorescence microscopy confirmed the uptake of the lipid nanoparticles by the nematode.

Sterilization of the nanoparticles is necessary since these nanoparticles were designed for medical application, more specifically for oral administration. Some processes that could be tested include filtration, autoclaving or ɣ-radiation. Further studies need to be performed to ensure that nor the antibiotic or lipid nanoparticle integrity are affected by the sterilization.

Antibacterial activity of the nanoparticles is another procedure that should be assessed.

Formulations also could be tested in other microorganisms such as *Pseudomonas aeruginosa*.

In conclusion, ciprofloxacin was successfully encapsulated in nanostructured lipid carriers and their efficacy was successfully tested in *C. elegans.*

7. References

1. Müller, R. Solid lipid nanoparticles (SLN) for controlled drug delivery: a review of the state of the art. *Eur. J. Pharm. Biopharm.* **50,** 161–177 (2000).

2. Wissing, S. A., Kayser, O. & Müller, R. H. Solid lipid nanoparticles for parenteral drug delivery. *Adv. Drug Deliv. Rev.* **56,** 1257–1272 (2004).

3. Tamjidi, F., Shahedi, M., Varshosaz, J. & Nasirpour, A. Nanostructured lipid carriers (NLC): A potential delivery system for bioactive food molecules. *Innov. Food Sci. Emerg. Technol.* **19,** 29–43 (2013).

4. Das, S. & Chaudhury, A. Recent advances in lipid nanoparticle formulations with solid matrix for oral drug delivery. *AAPS PharmSciTech* **12,** 62–76 (2011).

5. Uchechi, O., Ogbonna, J. D. N. & Attama, A. a. *Nanoparticles for Dermal and Transdermal Drug Delivery. Application of Nanotechnology in Drug Delivery* (2014).

6. Mäder, K. & Mehnert, W. Solid lipid nanoparticles: Production, characterization and applications. *Adv. Drug Deliv. Rev.* **47,** 165–196 (2001).

7. Garud, A., Singh, D. & Garud, N. Solid Lipid Nanoparticles (SLN): Method , Characterization and Applications. *Int. Curr. Pharm. J.* **1,** 384–393 (2012).

8. Müller, R. H., Radtke, M. & Wissing, S. A. Solid lipid nanoparticles (SLN) and nanostructured lipid carriers (NLC) in cosmetic and dermatological preparations. *Adv. Drug Deliv. Rev.* **54,** 131–155 (2002).

9. Kaur, S., Nautyal, U., Singh, R., Singh, S. & Devi, A. Nanostructure Lipid Carrier (NLC): the new generation of lipid nanoparticles. *Asian Pac. J. Heal. Sci.* **2,** 76–93 (2015).

10. Neupane, Y. R., Sabir, M. D., Ahmad, N., Ali, M. & Kohli, K. Lipid drug conjugate nanoparticle as a novel lipid nanocarrier for the oral delivery of decitabine: *ex vivo* gut permeation studies. *Nanotechnology* **24,** 1–11 (2013).

11. Schwarz, C., Mehnert, W., Lucks, J. S. & Müller, R. H. Solid lipid nanoparticles (SLN) for controlled drug delivery. I. Production, characterization and sterilization. *J. Control. Release* **30,** 83–96 (1994).

12. Sjöström, B., Westesen, K. & Bergenståhl, B. Preparation of submicron drug particles in lecithin-stabilized o/w emulsions. II. Characterization of cholesteryl acetate particles. *Int. J. Pharm.* **94,** 89–101 (1993).

13. Trotta, M., Debernardi, F. & Caputo, O. Preparation of solid lipid nanoparticles by a solvent emulsification-diffusion technique. *Int. J. Pharm.* **257,** 153–160 (2003).

14. Schubert, M. A. & Muller-Goymann, C. C. Solvent injection as a new approach for manufacturing lipid nanoparticles – evaluation of the method and process parameters. *Eur. J. Pharm. Biopharm.* **55,** 125–131 (2003).

15. Cortesi, R., Esposito, E., Luca, G. & Nastruzzi, C. Production of lipospheres as carriers for bioactive compounds. *Biomaterials* **23,** 2283–2294 (2002).

16. Gasco, M. R. Method for producing solid lipid microspheres having a narrow size distribution US Patent 5250236 A. (1997).

17. Mäder, K. & Mehnert, W. Solid lipid nanoparticles: production, characterization and applications. *Adv. Drug Deliv. Rev.* **47,** 165–96 (2001).

18. Mumper, R. J. & Jay, M. Microemulsions as precursors to solid nanoparticles US Patent 7153525 B1. (2006).

19. Battaglia, L. *et al. Techniques for the Preparation of Solid Lipid Nano and Microparticles. Application of Nanotechnology in Drug Delivery* (2014).

20. Koziara, J. M., Oh, J. J., Akers, W. S., Ferraris, S. P. & Mumper, R. J. Blood compatibility of cetyl alcohol/polysorbate-based nanoparticles. *Pharm. Res.* **22,** 1821–1828 (2005).

21. Pegi Ahlin Grabnar; Julijana Kristl; Jelka Šmid-Korbar. Optimization of procedure parameters and physical stability of solid lipid nanoparticles in dispersions. *Acta Pharm.* **48,** 259–267 (1998).

22. Kentish, S. *et al.* The use of ultrasonics for nanoemulsion preparation. *Innov. Food Sci. Emerg. Technol.* **9,** 170–175 (2008).

23. Kendall, G. What is Pharmaceutical Nanoemulsion? Available at: http://blogs.nottingham.ac.uk/malaysiaknowledgetransfer/2013/06/25/what-is-pharmaceutical-nanoemulsion/. (Accessed: 3rd October 2017)

24. McClements, D. J. & Rao, J. Food-grade nanoemulsions: formulation, fabrication, properties, performance, biological fate, and potential toxicity. *Crit. Rev. Food Sci. Nutr.* **51,** 285–330 (2011).

25. McClements, D. J. *Food Emulsions: Principles, Practices, and Techniques, Third Edition.* (2015).

26. Malvern instruments. *Zetasizer Nano Series User Manual. Department of Biochemistry Biophysics Facility , University of Chambridge* (2004).

27. Gaumet, M., Vargas, A., Gurny, R. & Delie, F. Nanoparticles for drug delivery: The need for precision in reporting particle size parameters. *Eur. J. Pharm. Biopharm.* **69,** 1–9 (2008).

28. Bunjes, H. & Unruh, T. Characterization of lipid nanoparticles by differential scanning calorimetry, X-ray and neutron scattering. *Adv. Drug Deliv. Rev.* **59,** 379–402 (2007).

29. Yadav, N., Khatak, S., Vir, U. & Sara, S. Solid lipid nanoparticles - a review. *Int. J. Appl. Pharm.* **5,** 8–18 (2013).

30. Physics, S. & August, R. The Theory of Ostwald Ripening. *J. Stat. Phys.* **38,** 231–252 (1985).

31. Freitas, C. & Müller, R. H. Spray-drying of solid lipid nanoparticles (SLN(TM)). *Eur. J. Pharm. Biopharm.* **46,** 145–151 (1998).

32. Jain, D. & Banerjee, R. Comparison of ciprofloxacin hydrochloride-loaded protein, lipid, and chitosan nanoparticles for drug delivery. *J. Biomed. Mater. Res. - Part B Appl. Biomater.* **86,** 105–112 (2008).

33. Ghaffari, S. *et al.* Ciprofloxacin Loaded Alginate/Chitosan and Solid Lipid Nanoparticles, Preparation, and Characterization. *J. Dispers. Sci. Technol.* **33,** 685–689 (2011).

34. Shah, M., Agrawal, Y. K., Garala, K. & Ramkishan, A. Solid lipid nanoparticles of a water soluble drug, ciprofloxacin hydrochloride. *Indian J. Pharm. Sci.* **74,** 434–42 (2012).

35. Shazly, G. A. Ciprofloxacin Controlled-Solid Lipid Nanoparticles : Characterization , In Vitro Release , and Antibacterial Activity Assessment. *Biomed Res. Int.* **2017,** (2017).

36. Cavalli, R. *et al.* Transmucosal transport of tobramycin incorporated in SLN after duodenal administration to rats. Part I—A pharmacokinetic study. *Pharmacol. Res.* **42,** 541–545 (2000).

37. Cavalli, R., Gasco, M. R., Chetoni, P., Burgalassi, S. & Saettone, M. F. Solid lipid nanoparticles (SLN) as ocular delivery system for tobramycin. *Int. J. Pharm.* **238,** 241–245 (2002).

38. Moreno-Sastre, M. *et al.* Pulmonary delivery of tobramycin-loaded nanostructured lipid carriers for *Pseudomonas aeruginosa* infections associated with cystic fibrosis. *Int. J. Pharm.* **498,** 263–273 (2016).

39. Wu, S.-S., Chein, C.-Y. & Wen, Y.-H. Analysis of ciprofloxacin by a simple high-performance liquid chromatography method. *J. Chromatogr. Sci.* **46,** 490–495 (2008).

40. National Center for Biotechnology Information. PubChem Compound Database. Available at: https://pubchem.ncbi.nlm.nih.gov/compound/2764. (Accessed: 10th November 2016)

41. National Center for Biotechnology Information. PubChem Compound Database. Available at: https://pubchem.ncbi.nlm.nih.gov/compound/36294 . (Accessed: 10th November 2016)

42. Cutting, G. R. Cystic fibrosis genetics: from molecular understanding to clinical application. *Nat. Rev. Genet.* **16,** 45–56 (2015).

43. Cystic Fibrosis Foundation. Patient Registry Annual Data Report 2015. *Bethesda, Maryl.* (2016).

44. Farrell, P. M. The prevalence of cystic fibrosis in the European Union. *J. Cyst. Fibros.* **7,** 450–453 (2008).

45. Rommens, J. M. *et al.* Identification of the Cystic Fibrosis Gene : Chromosome Walking and jumping. *Science (80-.).* **245,** 1059–1065 (1989).

46. Flume, P. A. & Van Devanter, D. R. State of progress in treating cystic fibrosis respiratory disease. *BMC Med.* **10,** 88 (2012).

47. Cantin, A. M., Hartl, D., Konstan, M. W. & Chmiel, J. F. Inflammation in cystic fibrosis lung disease: Pathogenesis and therapy. *J. Cyst. Fibros.* **14,** 419–430 (2015).

48. Döring, G., Flume, P., Heijerman, H. & Elborn, J. S. Treatment of lung infection in patients with cystic fibrosis: Current and future strategies. *J. Cyst. Fibros.* **11,** 461–479 (2012).

49. Mahenthiralingam, E., Urban, T. A. & Goldberg, J. B. The multifarious, multireplicon *Burkholderia cepacia complex* . **3,** 144–156 (2005).

50. Drevinek, P. & Mahenthiralingam, E. *Burkholderia cenocepacia* in cystic fibrosis : epidemiology and molecular mechanisms of virulence. *Clin. Microbiol. Infect.* **16,** 821–830 (2010).

51. Coutinho, C. P., Barreto, C., Cristino, M., Sa, I. & Sa, I. Incidence of *Burkholderia contaminans* at a cystic fibrosis centre with an unusually high representation of *Burkholderia cepacia* during 15 years of epidemiological surveillance. *J. Med. Microbiol.* **64,** 927–935 (2015).

52. Leitão, J. H. *et al.* Pathogenicity, virulence factors, and strategies to fight against *Burkholderia cepacia* complex pathogens and related species. *Appl. Microbiol. Biotechnol.* **87,** 31–40 (2010).

53. Diab, R., Khameneh, B., Joubert, O. & Duval, R. Insights in nanoparticle-bacterium interactions: New frontiers to bypass bacterial resistance to antibiotics. *Curr. Pharm. Des.* **21,** 4095–4105 (2015).

54. Gonzalez-Moragas, L., Roig, A. & Laromaine, A. *C. elegans* as a tool for *in vivo* nanoparticle assessment. *Adv. Colloid Interface Sci.* **219,** 10–26 (2015).

55. Ramos, C. G. & Leitão, J. H. *Caenorhabditis Elegans* as a Research Tool to Unveil Bacterial Virulence Determinants: Lessons from the *Burkholderia Cepacia* Complex. *Nematodes:*

Morphology, Functions and Management Strategies (2011).

56. Ewbank, J. J. Tackling both sides of the host – pathogen equation with *Caenorhabditis elegans* . *Microbes Infect.* **4,** 247–256 (2002).

57. Colmenares, D. *et al.* Delivery of dietary triglycerides to *Caenorhabditis elegans* using lipid nanoparticles: Nanoemulsion-based delivery systems. *Food Chem.* **202,** 451–457 (2016).

58. Wolkow, C.A. and Hall, D. H. Introduction to the Dauer Larva, Overview. In WormAtlas. Available at: http://www.wormatlas.org/dauer/introduction/DIntroframeset.html. (Accessed: 1st October 2017)

59. National Center for Biotechnology Information. PubChem Compound Database. Available at: https://pubchem.ncbi.nlm.nih.gov/compound/9920342. (Accessed: 6th December 2017)

60. National Center for Biotechnology Information. PubChem Compound Database. Available at: https://pubchem.ncbi.nlm.nih.gov/compound/5281955. (Accessed: 6th December 2017)

61. National Center for Biotechnology Information. PubChem Compound Database. Available at: https://pubchem.ncbi.nlm.nih.gov/compound/3893. (Accessed: 6th December 2017)

62. National Center for Biotechnology Information. PubChem Compound Database. Available at: https://pubchem.ncbi.nlm.nih.gov/compound/11005. (Accessed: 6th December 2017)

63. National Center for Biotechnology Information. PubChem Compound Database. Available at: https://pubchem.ncbi.nlm.nih.gov/compound/985 . (Accessed: 6th December 2017)

64. National Center for Biotechnology Information. PubChem Compound Database. Available at: https://pubchem.ncbi.nlm.nih.gov/compound/5281. (Accessed: 6th December 2017)

65. National Center for Biotechnology Information. PubChem Compound Database. Available at: https://pubchem.ncbi.nlm.nih.gov/compound/11006. (Accessed: 6th December 2017)

66. Brenner, S. The genetics of *Caenorhabditis elegans. Genetics* **77,** 71–94 (1974).

67. Richau, J. A. *et al.* Molecular Typing and Exopolysaccharide Biosynthesis of *Burkholderia cepacia* Isolates from a Portuguese Cystic Fibrosis Center. *J. Clin. Microbiol.* **38,** 1651–1655 (2000).

68. Darling, P., Chan, M. & Cox, A. D. Siderophore Production by Cystic Fibrosis Isolates of *Burkholderia cepacia. Infect. Imunity* **66,** 874–877 (1998).

69. Lopes, C. P. A. Development and Characterization of Lipid Nanoparticles prepared by Miniemulsion Technique. (2014).

70. Catarina, A. Development , Optimization and Characterization of Lipid Nanoparticles : Encapsulation of Lidocaine in Nanostructured Lipid Carriers. (2016).

71. Evrim, S., Tekkeli, K. & Sa, A. O. Spectrofluorimetric determination of tobramycin in human serum and pharmaceutical preparations by derivatization with fluorescamine. *Luminescence* **29,** 87–91 (2013).

72. Son, H. R. Comparison of New and Existing Spectrophotometric Methods for the Analysis of Tobramycin and Other Aminoglycosides. *J. Pharm. Sci.* **79,** 428–431 (1990).

73. Ungaro, F. *et al.* Dry powders based on PLGA nanoparticles for pulmonary delivery of antibiotics : Modulation of encapsulation efficiency, release rate and lung deposition pattern by hydrophilic polymers. *J. Control. Release* **157,** 149–159 (2012).

74.   The Pharmaceutics and Compounding Laboratory: Emulsions: Preparation and Stabilization. Available at: https://pharmlabs.unc.edu/labs/emulsions/hlb.htm. (Accessed: 5th October 2017)

75.   Keles, S., Kaygusuz, K. & Sarı, A. Lauric and myristic acids eutectic mixture as phase change material for low-temperature heating applications. *Int. J. energy Res.* **29,** 857–870 (2005).

76.   Tunc, K., Sari, A., Tarhan, S., Ergu, G. & Kaygusuz, K. Lauric and palmitic acids eutectic mixture as latent heat storage material for low temperature heating applications. *Energy* **30,** 677–692 (2005).

77.   Sari, A. & Kaygusuz, K. Thermal performance of a eutectic mixture of lauric acid and stearic acids as PCM encapsulated in the annulus of two concentric pipes. *Sol. energy* **72,** 493–504 (2002).

78.   Jeffrey B. Kaplan, Karen LoVetri, Silvia T. Cardona, Srinivasa Madhyastha, Irina Sadovskaya, Saïd Jabbouri, and E. A. I. Recombinant human DNase I decreases biofilm and increases antimicrobial susceptibility in staphylococci. *J Antibiot* **65,** 73–77 (2012).

79.   Stadler, M., Mayer, A., Anke, H. & Sterner, O. Fatty Acids and Other Compounds with Nematicidal Activity from Cultures of *Basidiomycetes*. *Planta Med* **60,** 128–132 (1993).

80.   Cardona, S. T., Wopperer, J., Eberl, L. & Valvano, M. A. Diverse pathogenicity of *Burkholderia cepacia* complex strains in the *Caenorhabditis elegans* host model. *Microbiol. Lett.* **250,** 97–104 (2005).

81.   Sousa, S. A., Ramos, C. G., Moreira, L. M. & Leitão, J. H. The hfq gene is required for stress resistance and full virulence of *Burkholderia cepacia* to the nematode *Caenorhabditis elegans*. *Microbiology* **156,** 896–908 (2010).

82.   FDA U.S Food and Drug Administration. Available at: https://www.fda.gov/default.htm. (Accessed: 5th October 2017)

8.   Appendix

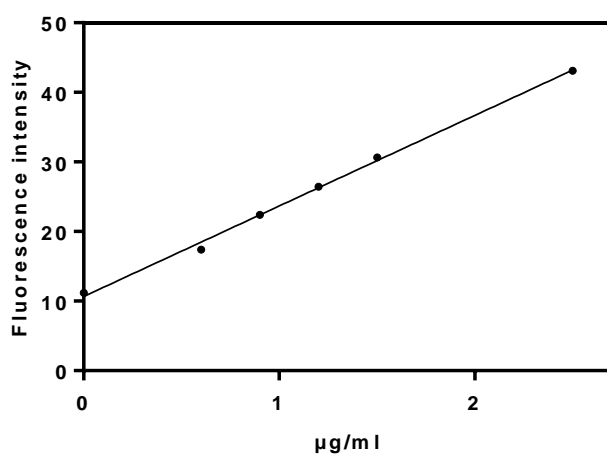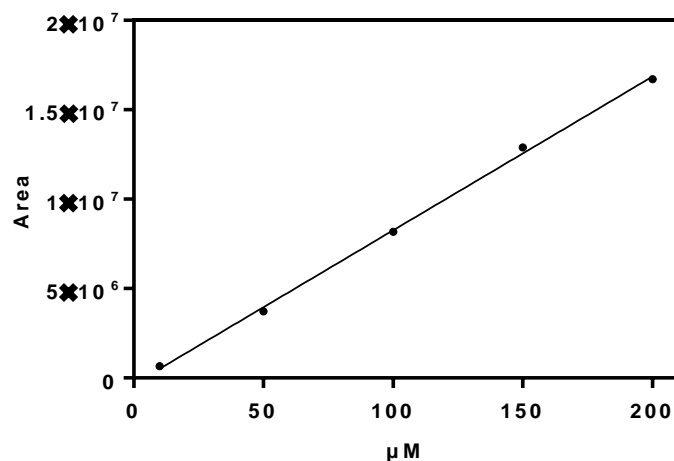**Annex 1**
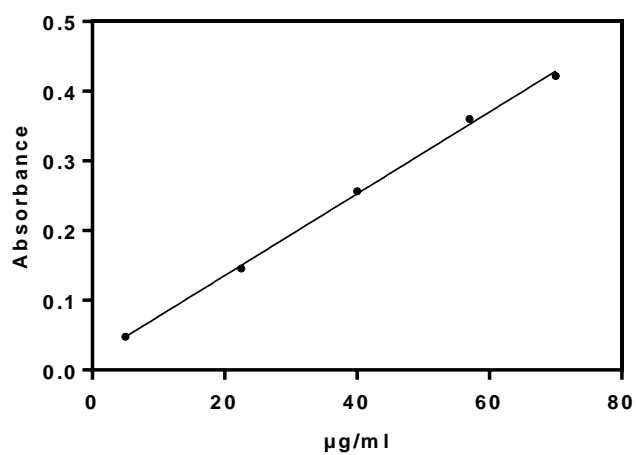
Figure a1: Calibration curve obtained for tobramycin. Equation of linear regression: Absorbance=0.0062µg/mL with a R square of 0.994.

Annex 2

Figure a2: Calibration curve obtained for tobramycin. Equation of linear regression: Fluorescence intensity =13.016µg/mL +10.663 with a R square of 0.9973.

Figure a3: Calibration curve obtained for ciprofloxacin. Equation of linear regression: Area=85998µM-342478 with a R square of 0.998.
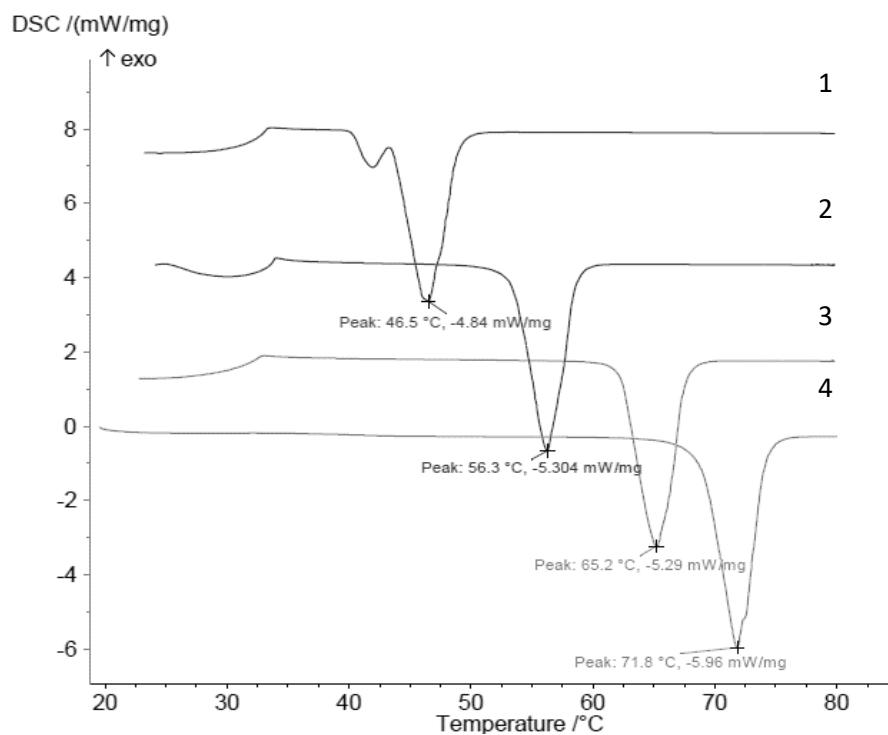
Annex 4

Table a1: Characterization in terms of size in nm, polydispersity index and zeta potential of the nanoparticles prepared with formulation NLC_1 to NLC_TOB.

| Formulation	Size (nm)	SD	PdI	SD	ZP (mV)	SD	pH	SD
NLC_1	219.0	11.0	0.400	0.04	-20,3	0.52	3.5	0.08
NLC_2	273.8	55.0	0.345	0.08	-52,6	3.47	5.93	0.29
NLC_3	668.1	232.6	0.840	0.08	-24,1	0.65	4.48	0.32
NLC_4	255.9	40.8	0.342	0.06	-56,9	3.72	5.53	0.34
NLC_5	205.6	17.9	0.196	0.07	-54,8	7.30	5.92	0.24
NLC_6	202.4	2.7	0.208	0.03	-47,5	0.90	6.16	0.21
NLC_7	246.3	1.6	0.350	0.02	-50,8	5.05	6.08	0.53
NLC_CIP	258.5	50.7	0.399	0.08	-48.9	4.09	6.14	0.15
NLC_TOB	255.3	63.5	0.325	0.09	-22.0	3.62	7.58	0.13

Annex 5

Figure a4: DSC thermal analysis of individual fatty acids. 1-Lauric acid; 2- Myristic acid; 3- Palmitic acid; 4-Stearic acid.

Annex 6
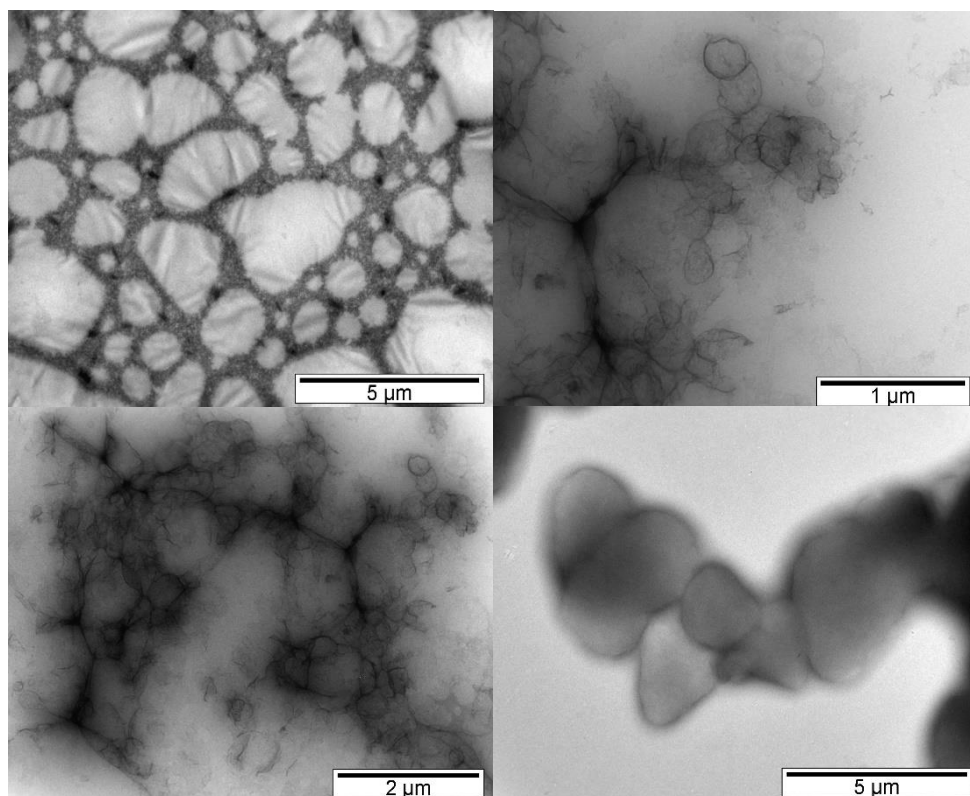
Figure a5: TEM images of empty nanoparticles (Formulation NLC_4) without filtration.